

**OPTIMIZATION OF SPRAY PARAMETERS FOR HIGH  
VELOCITY OXY-FUEL (HVOF) SPRAYED ABRADABLE  
COATING**

Thesis Report submitted in partial fulfillment of the requirements for the award of  
degree of

**Master of Engineering**  
in  
**PRODUCTION AND INDUSTRIAL ENGINEERING**

By:  
**Gaurav**  
(Roll no. 821082001)

Under the supervision of

**Mr. Devender Kumar**  
(Assistant Professor, MED, Thapar University Patiala)



Mechanical Engineering Department  
Thapar University, Patiala- 147004, India  
(Declared as Deemed-to-be university u/s 3 of the UGC Act, 1956)

## CERTIFICATE

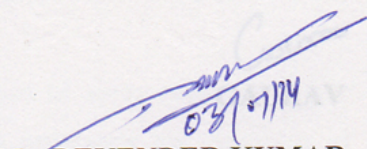
This is to certify that the work in this thesis report “**OPTIMIZATION OF SPRAY PARAMETERS FOR HIGH VELOCITY OXY-FUEL (HVOF) SPRAYED ABRADABLE COATING**” submitted in partial fulfillment of requirement for the award of **Master of Engineering Degree in Production & Industrial Engineering** in Mechanical Engineering Department of Thapar University, Patiala, is an authentic record of work carried out by me under the guidance of **Mr. Devender Kumar**, Assistant Professor, Mechanical Engineering Department, Thapar University, Patiala.

The matter embodied in this report has not been submitted in part or full to any university or institute for the award of any degree.

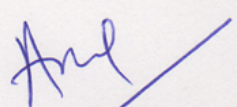
**Date:** 03/01/2014

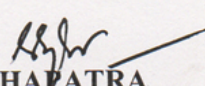
  
(GAURAV)

This is to certify that the above declaration made by the student concern is correct to the best of my knowledge and belief.

  
**Mr. DEVENDER KUMAR**  
Assistant Professor  
Deptt. of Mechanical Engg.  
Thapar University, Patiala

**Countersigned by:**

  
**Dr. AJAY BATISH**  
Head & Professor  
Deptt. of Mechanical Engg.  
Thapar University, Patiala

  
**Dr. S.K. MOHAPATRA**  
Dean of Academic Affairs  
Thapar University, Patiala

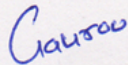
## ACKNOWLEDGEMENT

This thesis has been an inspiring, very challenging, but always interesting and exciting experience. In first place, I would like to express my sincere gratitude to my guide **Mr. Devender Kumar, Assistant professor, Department of Mechanical Engineering, Thapar University, Patiala** for acting as my thesis supervisor and giving valuable guidance, for the patience, encouragement, many fruitful discussions, and never giving up on me.

It is my proud privilege to express regards and sincere thanks to **Dr. Ajay Batish, Professor and Head, Mechanical Engineering Department, Thapar University, Patiala** for his invaluable guidance and support. I am highly thankful to **Dr. Ajay Malik**, Assistant professor, Mechanical Engineering Department UIET Kurukshetra for his invaluable guidance & continuous support.

Finally, I thanks to entire faculty and staff of Department of Mechanical Engineering, Thapar University, Patiala for their help, Inspiration and moral support, which went a long way in successfully completion of my thesis.

My special thanks to my family members and friends who constantly encouraged me to complete this study.

  
**GAURAV**

## **ABSTRACT**

Abradable coating acts as a seal between the blades and casing of aircraft or gas turbine engine. The clearance between the blades and casing should be as small as possible to increase the efficiency of turbine engine. Abradable coatings are engineered to minimize this gap and to enhance the engine performance. During its operation blade tips may rub the stationary casing due to either thermal expansion or misalignment, this will cause wear to blade tip. Abradable coatings act as sacrificial layer between blade and casing and are soft enough to avoid significant wear to blade tips. The coating should not only be soft enough to be scraped easily without damaging the blade tip (good abrasability) but also should have high resistance against erosion by the high speed gas flow and solid particles in gas (erosion resistance). Therefore the abrasability and the erosion resistance are the most important properties of the abrasable coating. But both properties are contradictory and the coating should provide a good balance between the abrasability and erosion resistance.

The thermal sprayed abrasable coatings has been used because of its simple manufacturing process, easy repair of the components, easy adjustment of its properties and good sealing effectiveness.

In this work, an attempt has been made to determine the influence of spray parameters like oxygen flow rate, fuel flow rate and spray angle on the erosion resistance and hardness of abrasable coating produced by HVOF (High Velocity Oxy-Fuel). Optimum values of these parameters are identified for attaining better erosion resistance and low hardness of coating by the application of Taguchi method.

## LIST OF CONTENTS

	Page No.
<b>CERTIFICATE</b>	<b>I</b>
<b>ACKNOWLEDGEMENT</b>	<b>II</b>
<b>ABSTRACT</b>	<b>III</b>
<b>LIST OF CONTENTS</b>	<b>IV</b>
<b>LIST OF FIGURES</b>	<b>VII</b>
<b>LIST OF TABLES</b>	<b>VIII</b>
<b>CHAPTER 1</b>	
<b>1 INTRODUCTION</b>	<b>1-13</b>
<b>1.1 Wear</b>	<b>2</b>
<b>1.2 Types of wear</b>	<b>2</b>
<b>1.2.1 Abrasive wear</b>	<b>3</b>
<b>1.2.2 Adhesive wear</b>	<b>3</b>
<b>1.2.3 Erosion wear</b>	<b>3</b>
<b>1.2.4 Corrosive wear</b>	<b>3</b>
<b>1.2.5 Fatigue wear</b>	<b>3</b>
<b>1.3 Erosion Wear</b>	<b>4</b>
<b>1.4 Mechanism of erosion wear</b>	<b>4</b>
<b>1.4.1 Cutting</b>	<b>4</b>
<b>1.4.2 Ploughing</b>	<b>5</b>
<b>1.4.3 Extrusion and forging</b>	<b>5</b>
<b>1.4.4 Subsurface deformation and cracking</b>	<b>6</b>
<b>1.5 Thermal spray coating</b>	<b>6</b>
<b>1.6 Methods of coating</b>	<b>6</b>
<b>1.6.1 High Velocity Oxy-Fuel (HVOF)</b>	<b>7</b>
<b>1.6.2 Plasma Spraying</b>	<b>8</b>

1.6.3	Arc Spray	8
1.7	Abradable coating	9
1.8	The Taguchi Method for design of experiment	10
1.9	Steps applied in Taguchi method	10
1.10	Signal to noise ratio and ANOVA approaches	12
1.11	Optimal design	12
1.12	Determination of confidence interval	13
<b>CHAPTER 2</b>		
<b>2</b>	<b>LITERATURE REVIEW</b>	<b>14-23</b>
<b>CHAPTER 3</b>		
<b>3</b>	<b>RESEARCH PROBLEM AND METHODOLOGY</b>	<b>24</b>
3.1	Gaps in Literature	24
3.2	Problem Formulation and research objective	24
<b>CHAPTER 4</b>		
<b>4</b>	<b>EXPERIMENTATION</b>	<b>25-37</b>
4.1	Design of Experiments	25
4.2	Steps applied in design of experiments	25
4.3	Substrate Material	26
4.4	Properties of substrate material	27
4.4.1	Chemical composition	27
4.4.2	Hardness	28
4.5	Steps followed for sample preparation	29
4.6	Coating	29
4.7	Coating powder	31
4.8	Test conducted	31
4.8.1	Erosion test	32
4.8.2	Parts of erosion testing machine	33
4.8.3	Experimentation parameters	36

<b>4.9</b>	<b>Rockwell superfacial Hardness test</b>	<b>37</b>
	<b>4.9.1 Rockwell Hardness scale</b>	<b>37</b>
<b>4.10</b>	<b>Erodent</b>	<b>37</b>

## CHAPTER 5

<b>5</b>	<b>RESULTS &amp; DISCUSSIONS</b>	<b>38-51</b>
<b>5.1</b>	<b>Analysis of erosion behaviour</b>	<b>38</b>
<b>5.2</b>	<b>Calculation of signal to noise ratio for response factors</b>	<b>39</b>
<b>5.3</b>	<b>Analysis of erosion for spray parameters</b>	<b>40</b>
	<b>5.3.1 Effect of input factors on erosion</b>	<b>40</b>
	<b>5.3.2 Analysis of variance of erosion</b>	<b>40</b>
<b>5.4</b>	<b>Optimum erosion rate</b>	<b>43</b>
<b>5.5</b>	<b>Analysis of hardness</b>	<b>44</b>
<b>5.6</b>	<b>Calculation of signal to noise ratio for response factors</b>	<b>45</b>
<b>5.7</b>	<b>Analysis of hardness for spray parameters</b>	<b>46</b>
	<b>5.3.1 Effect of input factors on hardness</b>	<b>46</b>
	<b>5.3.2 Analysis of variance for hardness</b>	<b>46</b>
<b>5.8</b>	<b>Optimum hardness</b>	<b>49</b>
<b>5.9</b>	<b>Experimental Validation</b>	<b>50</b>
<b>5.10</b>	<b>Discussion</b>	<b>51</b>

## CHAPTER 6

<b>6</b>	<b>CONCLUSIONS AND SCOPE FOR FUTURE WORK</b>	<b>52</b>
----------	--	-----------

	<b>REFERENCES</b>	<b>53</b>
--	-------------------	-----------

## LIST OF FIGURES

	Page No.	
Figure 1.1	Cutting Erosion	4
Figure 1.2	Ploughing Erosion	5
Figure 1.3	Extrusions and Forging Mechanism	5
Figure 1.4	Subsurface Deformation and Cracking	6
Figure 1.5	High Velocity Oxy-Fuel Spraying	7
Figure 1.6	Plasma Spraying	8
Figure 1.7	Arc Spraying	9
Figure 1.8	Steps in Taguchi Optimization	11
Figure 4.1	Photograph of substrate (uncoated)	27
Figure 4.2	Microhardness Tester	28
Figure 4.3	Indent on Specimen	28
Figure 4.4	Vickers Hardness number of specimen (uncoated)	28
Figure 4.5	High Velocity Oxy-Fuel Coating Machine	30
Figure 4.6	Photograph of Coated Samples	30
Figure 4.7	Erosion Testing Apparatus	32
Figure 4.8	Schematics of Erosion Testing Apparatus	33
Figure 4.9	Rockwell Superfacial principle	37
Figure 5.1	Main Effects plot for S/N Ratio	42
Figure 5.2	Main Effects plot for Data Means	42
Figure 5.3	Main Effects plot for S/N Ratio	48
Figure 5.4	Main Effects plot for Data Means	48

## LIST OF TABLES

	Page No.	
Table 4.1	Process Parameters and Their Levels	26
Table 4.2	Orthogonal Array	26
Table 4.3	Chemical composition of SuperCo-188	27
Table 4.4	Specimens Microhardness	29
Table 4.5	Properties of METCO 601 NS	31
Table 4.6	Control Parameters of Erosion Testing Apparatus	33
Table 4.7	Erosion Testing Machine parts	34
Table 4.8	Experimentation Parameters	36
Table 4.9	Rockwell Superficial Hardness scale	37
Table 5.1	Result of Erosion rates with 3 trials for each	38
Table 5.2	Calculation of S/N ratio for response Factors (MINITAB Output)	39
Table 5.3	Response table for S/N Ratio (MINITAB Output)	40
Table 5.4	Response table for Mean (MINITAB Output)	40
Table 5.5	ANOVA for S/N Ratio (MINITAB output)	41
Table 5.6	ANOVA for Mean (MINITAB output)	41
Table 5.7	Best Combination of Factor Levels	43
Table 5.8	Result of Hardness with 3 trials for each	44
Table 5.9	Calculation of S/N ratio for response Factors (MINITAB Output)	45
Table 5.10	Response Table for S/N Ratio (MINITAB Output)	46
Table 5.11	Response Table for Mean (MINITAB Output)	46
Table 5.12	ANOVA for S/N Ratio (MINITAB output)	47
Table 5.13	ANOVA for Mean (MINITAB output)	47
Table 5.14	Best Combination of Factor Levels	49
Table 5.15	Predicted Optimal Values, Confidence Intervals and Results of Confirmation Experiments	50

Surface modification is an important term which can be helpful for achieving increased reliability and enhanced performance of industrial components. The increased requirement for higher efficiency and reliability across the entire spectrum of manufacturing and engineering industries has ensured that most modern-day components are subjected to increasingly bad environments during routine operation.

Metallic surfaces are exposed to a variety of environments in which metal loss occurs by processes other than chemical-electrochemical (e.g. corrosion) [1]. Examples of such processes are abrasive wear, impact erosion and arc erosion, in which metal is mechanically removed from the surface by mechanical and/or thermal driving forces leading to rupture of the surface layers from the bulk metal. The various critical components are therefore, subjected to more rapid degradation and the components parts fail to withstand the changing and heavy operating conditions and this has been taking a decreasing of industry's economy. In an large number of cases, the increased damage of parts and their eventual failure have been traced due to material damage brought about by their environments and also by high relative motion between mating surfaces, cyclic stresses, corrosive media, extreme temperature etc. [3]. Impact erosion can, for example, be a serious problem for turbine engines operated in sandy and dusty environments [1].

Thus, a protective coating is used between the surfaces of the component and the aggressive environment and it is act as a barrier between surface and environment [2]. It is now generally accepted practice to apply coatings to the surfaces of components when protection is required against surface degradation processes such as wear, fretting, oxidation, corrosion and erosion [5-24]. The coated materials then function together as a degradation resistant composite system. Coatings are used on components in the compressor, combustion chamber and turbine engine sections [3]. In addition to their use as surface protection systems, coatings are also used for sealing (clearance control) applications in the compressor and turbine [5]. It is advantageous and accepted globally to be an attractive means to significantly reduce damage to the actual component by acting as the first line of defense. Coatings have widely used to give protection against erosion and corrosion of parts and is to protect the material from chemical and physical interaction with its inside and outside environment [7].

The main requirement for coating industrial component with a coating material lies on the following needs:

1. To improve the functional performance of component [35-37].
2. To improve the component life by reducing wear due to erosion and abrasion [8].
3. To improve the component life by rebuilding the worn part to its original dimensions [29].
4. To improve the function of a low-cost material by coating their surface with a high performance coating [31].

## **1.1 WEAR**

Wear is defined by the American Society for Testing and Materials (ASTM) as damage to a solid surface, generally involving the progressive loss of material, due to relative motion between that surface and a contacting substance or substances. The wear damage may be in the form of micro-cracks or localized plastic deformation. Wear is a complex phenomenon in which real contact area between two solid surfaces compared with the apparent area of contact is invariably very small, being limiting to the points of contact between surface asperities. The load applied to the surfaces will be transferred through these points of contact and the localized forces can be very large. Wear to be produced not only by rubbing contact with a solid surface, but also by particles, liquids, electric arcs or gas streams [12]. The material intrinsic surface properties, the surface finish, load, speed and temperature and properties of the opposing surfaces are important in determining the wear rate [13]. Wear, the progressive loss of substance from the operating surfaces of the mechanically interacting element of a tribo-system may be measured in terms of weight loss or volume loss [29-37].

## **1.2 TYPES OF WEAR**

A number of different wear phenomena are commonly encountered and presented in the literature. Wear mechanisms do not necessarily act independently and wear mechanisms are not mutually exclusive. Wear mechanisms frequently overlap and occur in a synergistic manner, producing a greater rate of wear than the sum of the individual wear mechanisms. Some commonly referred to wear mechanisms (or processes) include:

- 1.2.1) Abrasive wear
- 1.2.2) Adhesive wear
- 1.2.3) Erosion wear
- 1.2.4) Corrosive wear
- 1.2.5) Fatigue wear

### **1.2.1) Abrasive Wear**

Abrasive wear can be defined as wear that occurs when a hard surface slides against and cuts groove from a softer surface. It may account for most failures in practice. Hard particles or asperities which cut or groove one of the rubbing surfaces produce abrasive wear [13].

### **1.2.2) Adhesive Wear**

Adhesive wear can be defined as wear due to localized bonding between contacting solid surfaces leading to material transfer between the two surfaces or the loss from either surface. For occurrence of adhesive wear it is necessary for the surfaces to be in intimate contact with each other. Surfaces which are held apart by lubricating film, oxide film etc. reduces the tendency for adhesion to occur [13].

### **1.2.3) Erosive Wear**

Erosive wear can be defined as the process of metal removal due to impingement of solid particles on the surface. Erosion is caused by a gas or a liquid, which may or may not carry the entrained solid particles, impinging on the surface. When the angle of impingement is small, the wear produced is closely analogy to abrasion. When the angle of impingement is normal to the surface, material is displaced by the plastic flow or is dislodged by the brittle failure.

### **1.2.4) Surface Fatigue Wear**

Wear of a solid surface caused by fracture arising from material fatigue. The term 'fatigue' is broadly applied to the failure phenomenon where a solid is subjected to cyclic loading involving tension and compression above a certain critical stress. Repeated load causes the generation of micro cracks at the site of a pre-existing point of weakness. On subsequent loading and unloading, the micro cracks propagate. Once the crack reaches the critical size, it changes its direction to emerge at the surface, and thus flat sheet like particles is detached at the time of wearing. The number of stress cycles required to cause such failure decreases as the corresponding magnitude of stress increases. Vibrations are a common cause of fatigue wear.

### **1.2.5) Corrosive Wear**

Most metals are thermodynamically unstable in air and react with oxygen to form an oxide, which usually develop layer or scales on the surface of metal or alloys when their interfacial bonds are poor. Corrosion wear is the gradual eating away or deterioration of unprotected metal surfaces by the effects of the atmosphere, acids, gases etc [13]. This type of wear creates pits and perforations and may eventually dissolve metal parts.

### 1.3 EROSION WEAR

Erosion wear is the dominant process which can be defined as the removal of material from a solid surface. It is due to mechanical interaction between the surface and the impinging particles in a liquid stream. In Erosion process there is a transfer of kinetic energy to the surface. With the increase in kinetic energy of the particles impacting at the target surface, it leads to increase in the material loss due to erosion. It depends on the predominant impact angle of particle impingement with the material surface and it will vary from  $0^{\circ}$  to  $90^{\circ}$  [18]. Impact angle depend on both fluid particle and particle-particle interaction. This type of wear can be practically found in slurry pumps, angled pipe bends, turbines, pipes and pipe fitting, nozzles, burners etc. The material loss due to erosion increases with the increase in kinetic energy of the particle impacting at the target surface. The volume loss due to erosion is a troublesome problem for slurry transportation systems e.g. mineral transport systems, ash disposal systems etc. The erosion wear due to the air borne particles in some devices such as jet planes and turbines is also significant due to very high impact velocity [5].

### 1.4 MECHANISM OF EROSION WEAR

Erosion wear depends on impact angle, impact velocity, erodent material, erodent shape and size, carrier fluid and target material [6-9]. Both ductile and brittle material show different erosion wear mechanism. The commonly known erosion mechanisms are classified as:

1.4.1) Cutting

1.4.2) Ploughing

1.4.3) Extrusion and forging

1.4.4) Subsurface deformation and cracking

#### 1.4.1) Cutting Erosion

The cutting wear occurs when a hard material remove the material from the surface of the soft substrate material.

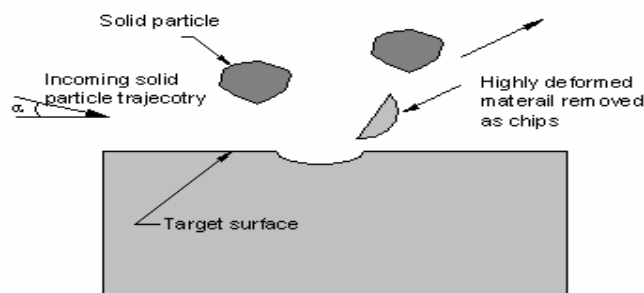


Figure 1.1 Cutting Erosion<sup>[12]</sup>

Cutting mechanism occurs when the impacting solid material strike the softer material at positive rake angle and remove the material from the target surface. The cutting mechanism is shown in figure 1.1

#### 1.4.2) Ploughing Erosion

The ploughing wear takes place when the solid particles struck the target substrate material at negative rake angle which results in the shearing of the substrate material. By this shearing the lip mechanism is formed on the substrate surface. The ploughing mechanism is shown in figure 1.2.

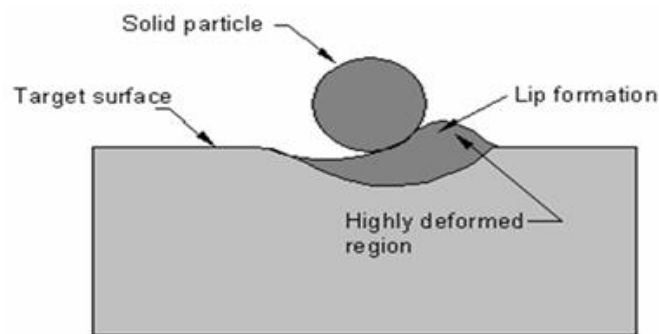


Figure 1.2 Ploughing Erosion<sup>[12]</sup>

#### 1.4.3) Extrusion and Forging Mechanism

In extrusion and forging mechanism of erosion wear the impact of a solid particle spreads the target material over the adjacent crater in the direction of impact. This spread material get further flattened and extended to develop a platelet, so it is also known as platelet mechanism. A proposed sequence of platelet mechanism is shown in figure 1.3.

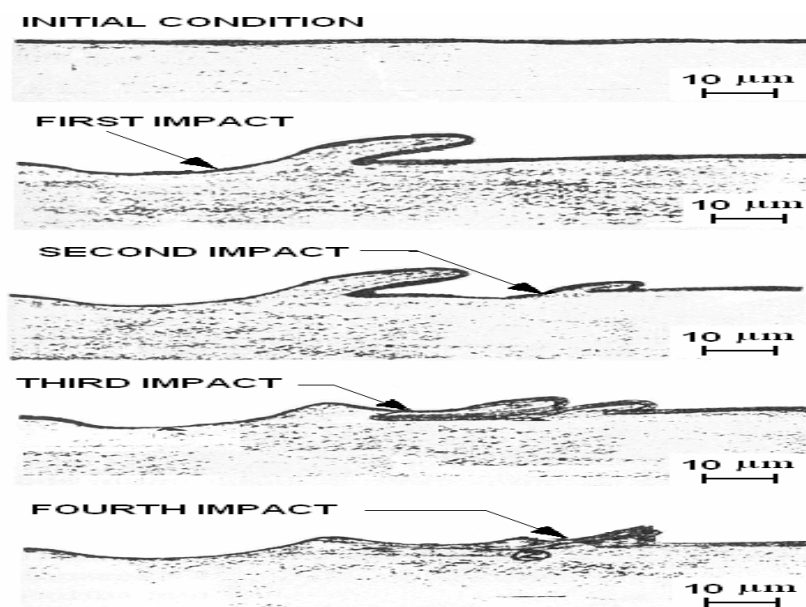


Figure 1.3 Extrusion and Forging Mechanism<sup>[13]</sup>

#### 1.4.4) Subsurface deformation and Cracking

This type of erosion mechanism occurs when solid particles impacted on the surface of the substrate due to the high velocity plastic deformation of the substrate. The plastic deformation of the substrate material results in crater and crack formation which causes brittle fracture of the specimen. The subsurface deformation and cracking is shown in figure.

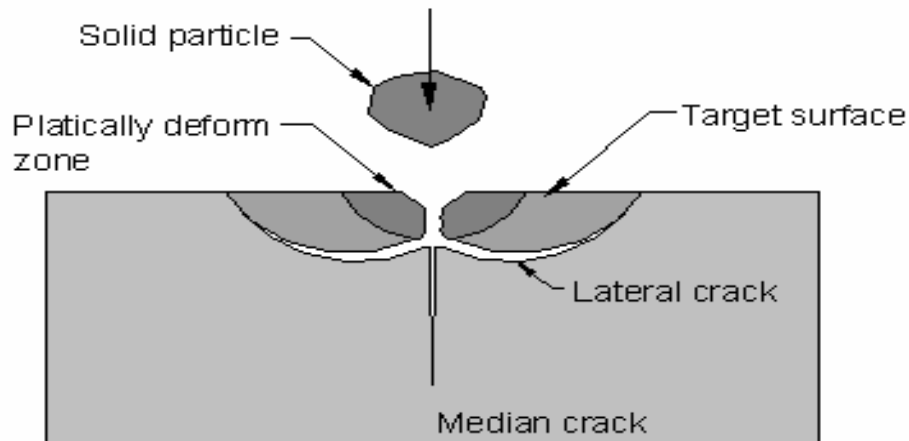


Figure 1.4 Subsurface Deformation and Cracking<sup>[13]</sup>

### 1.5 THERMAL SPRAY COATING

Coating is a covering that is applied on the surface of an object, usually as the substrate [33]. Coatings are applied to improve surface properties of the substrate, such as appearance, adhesion, corrosion resistance, wear resistance, and scratch resistance [20]. Coating may be applied as solids, liquids or gases. The thermal spray coating process is one of the most successful of all the advanced coating techniques because of the wide range of coating materials and substrates to which it can be applied. Metals and carbides are mostly used as base materials, although spraying of polymers has also been researched. A variety of engineering problems have been solved using the thermal spraying technique and research is ongoing to increase its application. The current field of application of thermal spraying includes; the oil industry to protect component surface against hostile environment, automotive industry, and the space exploration industry

### 1.6 METHODS OF COATING

1.6.1) High velocity oxygen fuel (HVOF)

1.6.2) Plasma spraying

1.6.3) Arc spray

### 1.6.1 High Velocity Oxy-Fuel (HVOF)

In HVOF a mixture of gaseous or liquid fuel and oxygen is fed into a combustion chamber, where they are ignited and combusted continuously. The resultant hot gas at a pressure close to 1 MPa emanates through a converging–diverging nozzle and travels through a straight section. The fuels can be gases (hydrogen, methane, propylene, acetylene, natural gas, etc.) or liquids (kerosene, etc.). The jet velocity at the exit of the barrel (>1000 m/s) exceeds the speed of sound. A powder feed stock is injected into the gas stream, which accelerates the powder up to 800 m/s. The stream of hot gas and powder is directed towards the surface to be coated. The powder partially melts in the stream, and deposits upon the substrate [28]. HVOF thermal spray provides an efficient way for depositing coatings of micro/nanostructured materials because of the powder particles hit the substrate with relatively high speed [31].

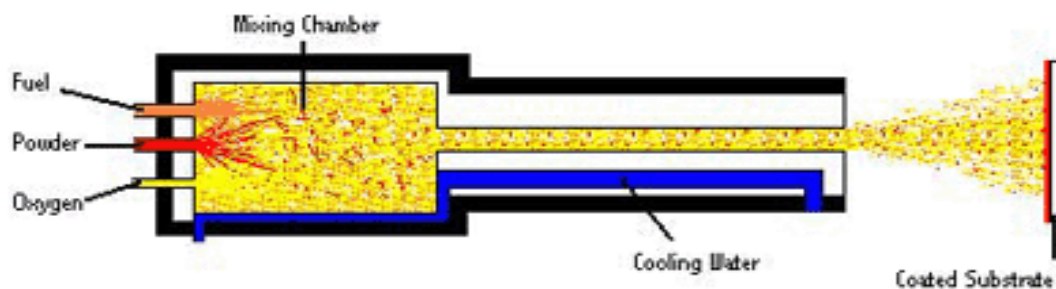


Figure 1.5 High Velocity Oxy-Fuel Spraying<sup>[24]</sup>

HVOF is one of the most versatile methods available for coating material and the resulting coating has low porosity and high bond strength. Advantages of this spraying technique include good substrate coating adhesion and high coating density. It is applicable to both metals and ceramics [18-21]. It involves the less setup cost as compared to other thermal spraying processes [24]. HVOF spraying is a very complex process, which has a large variety of variables affecting the deposit formation and hence coating properties. These variables include hardware characteristics (e.g., nozzle geometry and spraying distance) and process parameters, e.g., fuel gas, gas flow density, and powder feedstock. In the spray process, the powder particles experience very high speed combined with fast heating up to its melting point or above. This high temperature may cause evaporation of the powder or some components of it, dissolution, and phase transformations. Due to this complex nature of HVOF technique, the control and optimization of the process in order to achieve coating with desired properties is a highly challenging task.

### 1.6.2) Plasma Spraying

Plasma spray deposition or plasma spraying is a process that combines the particle melting, consolidation and quenching in a single operation. The process involves injection of powder particles (metallic, ceramic or cermets powders) into the plasma jet created by heating an inert gas in an electric arc confined within a water-cooled nozzle [10]. The temperature at the core of the plasma jet is 10,000 to 15,000 K. The particles injected into the plasma jet undergo rapid melting and at the same time are accelerated. These molten droplets moving at high velocities (exceeding 100 meters/second) impact on the surface of the substrate forming adherent coating. The coating is incrementally built up by impact of successive particles by the process of cooling, flattening and solidification. By virtue of the high cooling rates, typically  $10^5$  to  $10^6$  K/sec., the resulting microstructures are fine-grained and homogeneous. Plasma spraying has certain unique advantages over other competing surface engineering techniques [10]. By virtue of the high temperature (10,000- 15,000K) and high enthalpy available in the thermal plasma jet, any powder which melts without sublimation or decomposition, can be coated keeping the substrate temperature as low as  $50^{\circ}$  C. The coating process is fast and the thickness can go from a few tens of microns to a few mm.

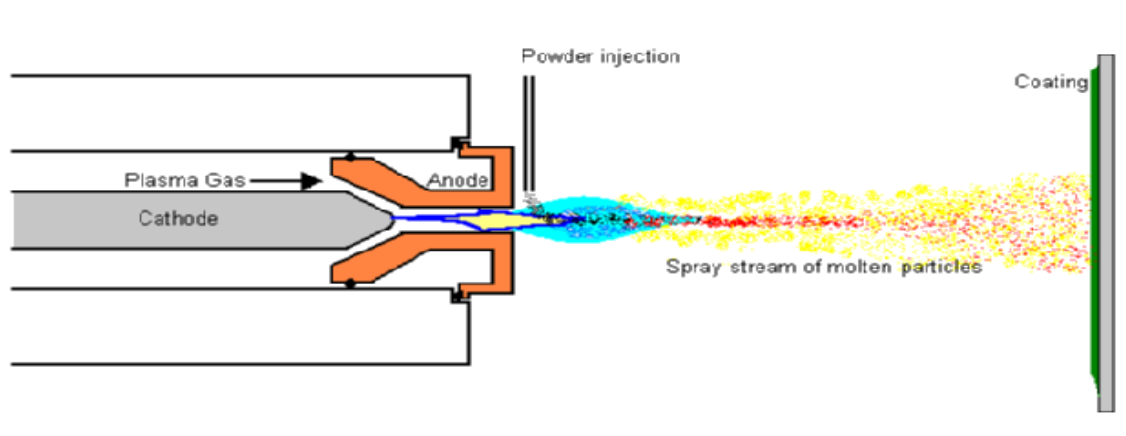


Figure 1.6 Plasma Spraying <sup>[10]</sup>

Plasma spraying is extensively used in hi-tech industries like aerospace, nuclear energy as well as Conventional industries like chemicals, textiles, plastics and paper mainly as wear resistant coatings in crucial components [16].

### 1.6.3) Arc Spraying

Two wires of desired materials act as electrodes when they are fed through a spray gun. The gun is connected to a high-current (DC) power source to facilitate an arc between them. An air stream through the back of the gun atomizes and propels the molten particles towards a

prepared surface. With adjustable parameters including voltage and amperage arc temperatures can reach 5000° C, enough to melt any material, at the same time the part surface remains cool. The process is considered energy efficient because all of the input energy is used to melt the spray materials.

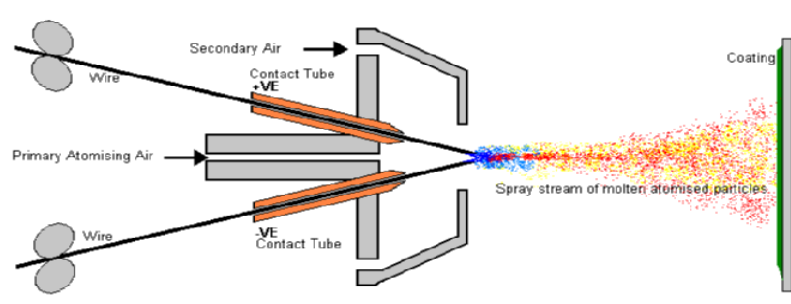


Figure 1.7 Arc Spraying<sup>[10]</sup>

## 1.7 ABRADABLE COATING

An abradable coating is that coating which is made of an abradable material meaning if it rubs against a more abrasive material in motion, the former will be worn out whereas the latter will face no wear. These coatings generally consist of a metallic and a non-metallic phase, and contain relatively high porosity levels [17]. Abradable coatings are used in aircraft jet engines in the compressor and turbine sections where a minimal clearance is needed between the blade tips and the casing [11-17]. In turbo machinery, the clearance between blade tips and the casing must account for thermal expansion as well as changes in concentricity due to shock loading events [25]. To prevent catastrophic tip to contact of casing, conservatively high clearances must be employed. But due to this large clearance more gases escape over the tip of the blades which increase the specific fuel consumption [24]. But the jet engine manufacturers strongly contributed towards this by increasing engine efficiency and power generation. One of the last means to increase the efficiency is the reduction of the clearance between the blade tip and casing [9-10]. This increase in efficiency can save the airlines significant operating costs [10].

The reduction of the blade tip to casing clearance can result in the blades rubbing against the shroud. By coating the shroud with an abradable, however, this interaction can be tolerated [25]. The rotating blades cut a groove in the abradable coating which reduces the clearance between blade tip and casing. A good abradable accommodates different wear mechanisms created by changing rub conditions mainly by blade's material, temperature, blade tip velocity and the incursion rate. The role of abradable coatings is not only to allow for closer

clearances, but automatically adjust clearances. Abradables are not restricted to aero engines. They can be used in most rotating machinery such as stationary gas turbine, turbo compressor, radial compressor and turbo charger [25].

The thermal sprayed abrasible coating has been used because of its simple manufacturing process. Also it can provide thermal barrier for the casing and reduce the influence of high temperature fuel gas on the casing [17].

## **1.8 THE TAGUCHI METHOD FOR DESIGN OF EXPERIMENT**

The quality engineering methods of Dr. Taguchi, employing design of experiments (DOE), is one of the most important statistical tools of TQM for designing high quality systems at reduced cost. Taguchi methods provide an efficient and systematic way to optimize designs for performance, quality, and cost. Fundamentally, traditional experimental design procedures are too complicated and not easy to use. A large number of experimental works have to be carried out when the number of the process parameters increases. To solve this problem, the Taguchi method uses a special design of orthogonal arrays to study the entire parameter space with only a small number of experiments. Taguchi methods has been widely utilized in engineering analysis and consists of a plan of experiments with the objective of acquiring data in a controlled way and in order to obtain information about the behaviour of a given process. The greatest advantage of this method is to save the effort in conducting experiments. Therefore, it reduces the experimental time as well as the cost by finding out significant factors fast [38].

## **1.9 STEPS APPLIED IN TAGUCHI METHODS**

Taguchi proposed a standard procedure for applying his method for optimizing any process. The steps suggested by Taguchi are:

### **1.9.1) Determine the quality characteristic to be optimized**

The first step in the Taguchi method is to determine the quality characteristic to be optimized. The quality characteristic is a parameter whose variation has a critical effect on product quality. It is the output or the response variable to be observed.

### **1.9.2) Identify the noise factors and test conditions**

The next step is to identify the noise factors that can have a negative impact on system performance and quality. Noise factors are those parameters which are either uncontrollable or are too expensive to control. Noise factors include variations in environmental operating

conditions, deterioration of components with usage, and variation in response between products of same design with the same input

**1.9.3) Identify the control parameters and their alternative levels**

The third step is to identify the control parameters thought to have significant effects on the quality characteristic. Control (test) parameters are those design factors that can be set and maintained. The levels (test values) for each test parameter must be chosen at this point.

**1.9.4) Design the matrix experiment and define the data analysis procedure**

The next step is to design the matrix experiment and define the data analysis procedure. First, the appropriate orthogonal arrays for the noise and control parameters to fit a specific study are selected. Taguchi provides many standard orthogonal arrays and corresponding linear graphs for this purpose. After selecting the appropriate orthogonal arrays, a procedure to simulate the variation in the quality characteristic due to the noise factors needs to be defined. Taguchi proposes orthogonal array based simulation to evaluate the mean and the variance of a product’s response resulting from Variations in noise factors.

**1.9.5) Conduct the matrix experiment**

The next step is to conduct the matrix experiment and record the results. The Taguchi method can be used in any situation where there is a controllable process. The controllable process can be an actual hardware experiment, systems of mathematical equations, or computer models that can adequately model the response of many products and processes.

**1.9.6) Analyze the data and determine the optimum levels for control factors**

After the experiments have been conducted, the optimal test parameter configuration within the experiment design must be determined. To analyze the results, the Taguchi method uses a statistical measure of performance called signal to noise (S/N) ratio borrowed from electrical control theory.

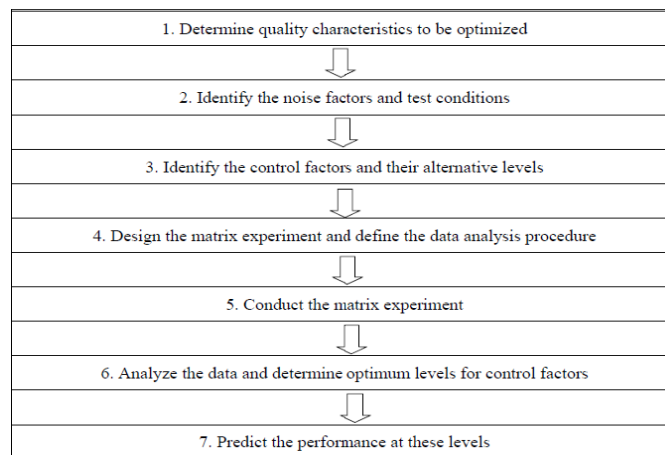


Figure 1.8 Steps in Taguchi Optimization

## 1.10 SIGNAL TO NOISE RATIO AND ANOVA APPROACHES

The S/N ratio developed by Dr. Taguchi is a performance measure to choose control levels that best cope with noise. The signal-to-noise (S/N) ratio measures how the response varies relative to the nominal or target value under different noise conditions [30]. You can choose from different S/N ratios, depending on the goal of your experiment. The S/N ratio takes both the mean and the variability into account. In its simplest form, the S/N ratio is the ratio of the mean (signal) to the standard deviation (noise). The S/N equation depends on the criterion for the quality characteristic to be optimized. While there are many different possible S/N ratios, three of them are considered standard and are generally applicable in the situations below [30]

### (i) Smaller-The-Better:

Smaller is better is used when the goal is to minimize the response and data is non negative with a target value of zero. The generic form of S/N ratio then becomes,

$$S/N = -10 \log \{ \Sigma (Y^2)/n \}$$

### (ii) Larger-The-Better:

Larger is better is used when the goal is to maximize the response and data is positive. The generic form of S/N ratio then becomes,

$$S/N = 10 \log \{ \Sigma (1/Y^2)/n \}$$

### (iii) Nominal-The-Best:

Nominal is best is used when the goal is to target the response and data is positive, zero or negative. The generic form of S/N ratio then becomes,

$$S/N = 10 \log (s^2)$$

ANOVA evaluate the importance of one or more factors by comparing the response variable means at the different factor levels.

## 1.11 OPTIMAL DESIGN

After determination of the optimum condition, the mean of the response ( $\mu$ ) at the optimum condition is predicted. The mean is estimated only from the significant parameters. The ANOVA identifies the significant parameters. Suppose, parameters A and B are significant and A<sub>2</sub>B<sub>2</sub> (second level of A=A<sub>2</sub>, second level of B=B<sub>2</sub>) is the optimal treatment condition. Then, the mean at the optimal condition (optimal value of the response characteristic) is estimated as [38]

$$\begin{aligned} \mu &= \bar{T} + (\bar{A}_2 - \bar{T}) + (\bar{B}_2 - \bar{T}) \\ &= \bar{A}_2 + \bar{B}_2 - \bar{T} \end{aligned}$$

Where  $\bar{T}$  = Overall mean of the response

$\overline{A}_2, \overline{B}_2$  = Average values of response at the second levels of parameters A and B respectively. It may also so happen that the prescribed combination of parameter levels (optimal treatment condition) is identical to one of those in the experiment. If this situation exists, then the most direct way to estimate the mean for that treatment condition is to average out all the results for the trials which are set at those particular levels.

### 1.12 DETERMINATION OF CONFIDENCE INTERVAL

The estimate of the mean ( $\mu$ ) is only a point estimate based on the average of results obtained from the experiment. Statistically this provides a 50% chance of the true average being greater than  $\mu$ . It is therefore customary to represent the values of a statistical parameter as a range within which it is likely to fall, for a given level of confidence. This range is termed as the confidence interval (CI). In other words, the confidence interval is a maximum and minimum value between which the true average should fall at some stated percentage of confidence.

The following type of confidence interval is suggested by Taguchi in regards to the estimated mean of the optimal treatment condition around the estimated average of a treatment condition predicted from the experiment.

The 95% confidence interval of confirmation experiments ( $CI_{CE}$ ) is calculated by using the equation as follows [38]:

$$CI_{CE} = \sqrt{F_{\alpha}(1, f_e) V_e \left[ \frac{1}{n_{eff}} + \frac{1}{R} \right]}$$

The 95% confidence interval of population ( $CI_{POP}$ ) is calculated by using the equation as follows [38]:

$$CI_{POP} = \sqrt{\frac{F_{\alpha}(1, f_e) V_e}{n_{eff}}}$$

Where,  $F_{\alpha}(1, f_e)$  = The F-ratio at the confidence level of  $(1-\alpha)$  against DOF 1 and error degree of freedom  $f_e$

$f_e$  = error DOF,

$$n_{eff} = \frac{N}{1 + [\text{DOF associated in the estimate of mean response}]}$$

$N$  = Total number of results,  $R$  = sample size for conformation experiment

[1] **Ashok K.Vijh (1977)** studied the wear mechanism and found that metals exhibit similar relative tendencies to metal loss by abrasive wear, impact erosion or arc erosion. High metal-metal bond energies in metals indicate high resistance to metal loss by any of these three processes.

[2] **Thomas E.Strangman (1985)** showed the benefits of thermal barrier coatings in the reduction of heat transferred into air-cooled components. Other potential benefits include increased resistance to hot corrosion, erosion and oxidation. Process-microstructure relationships are considered to be key factors in the achievement of thermal barrier coatings durability. Micro structural requirements for strain tolerance for both plasma-sprayed and electron beam physically vapor-deposited TBC systems were discussed. The effect of processing on bond coating oxidation and durability was also reviewed.

[3] **J.E.Restall et al. (1987)** investigated that the particulate materials ingested with the intake air, together with other solids generated within the gas turbine, are known to have the potential of degrading the hot oxidized or corroded surfaces of static and rotating aerofoil components. The nature of the degradation may be primarily by oxidation, corrosion or erosion or through some form of interaction between these processes. These regimes were illustrated by reference to the metallurgical assessment of components withdrawn from a marine gas turbine and a turbine used for pressurized fluidized-bed combustion trials. The conditions under which surface coatings may be expected to enhance the erosion-corrosion resistance of hot-end turbine components were discussed. From laboratory erosion experiments, particular attention was directed towards the importance of oxide scale plasticity and the ductile-to-brittle transition temperature of the coating.

[4] **S.Turenne et al. (1988)** performed slurry erosion to evaluate the effect of sand concentration on the erosion rate. By keeping the slurry velocity constant, different particle fluxes were obtained by varying the sand concentration in the slurry. The erosion tests were done with an erosion machine which gave a narrow slurry jet with a velocity of 17 m/s. The slurry jet was always oriented toward the surface at a normal incidence angle. It was observed that the erosion rate decreased according to a power law of the sand concentration in the slurry. The effect can be attributed to the flow conditions near the surface giving rise to rebounding particles which protect the surface from incident particles.

[5] **T.N. Rhys-Jones (1990)** described the range of thermal spraying processes available for the deposition of surface coatings for compressor, combustion chamber and turbine section components in aero engines. Typical coating applications were also discussed. Combustion flame, arc wire, high velocity combustion and plasma spraying techniques were described, and coatings for wear, oxidation and corrosion resistance, clearance control and thermal barrier applications were investigated.

[6] **Randall et al. (1991)** tested the erosion rates of cylindrical steel specimens at a constant speed of 18.7 m/s in an erosion pot tester using 1.2 wt.% suspension of SIC in oil for particle diameters between 20 and 500  $\mu\text{m}$ . The rate of particle impact on unit area of the surface at the stagnation line of erosion specimens was established as a function of particle size by short-time erosion tests, allowing a calculation of the mean mass removed for each particle impact as a function of particle size. Results showed that the decrease in erosion rate with decreasing particle size for suspensions of constant solids loading reflects the decrease in the proportion of particles impacting the target surface as well as the decrease in impact velocity.

[7] **L.Swadzba et al. (1993)** compared test results of protective properties of several coatings for aircraft engine compressor blades. Erosion and corrosion tests for the base metals and coatings were carried out. Corrosion test for base materials and anodic coating was made in neutral salt spray. For cathodic coatings a modified corrosion test was performed. It has been determined that the coatings obtained by physical vapour deposition (PVD), particularly (Ti, Al) and TiN(Pt) were the best in the erosion and corrosion test conditions. The electroplated Ni—Cd coatings do not show satisfactory erosion resistance, but they have good corrosion resistance. He showed that PVD coatings fulfill the requirements for the protection of aero engine compressor blades.

[8] **K.T.Kembaiyan et al. (1995)** described that the thermally sprayed tungsten carbide based coating offers an avenue to minimize severe fluid erosion, wear and corrosion encountered on drill bits and down hole tool assemblies used in mining, oil and gas drilling. The application of high rotary speeds and weights, presence of corrosive elements in the drilling muds, and high velocity mud with entrained cuttings subject these tools and drill bits to severe wear, erosion and corrosion and limit their service life. He described the successful application of thermally sprayed coatings in minimizing the fluid erosion, abrasive wear and corrosion in three cone and polycrystalline diamond bits. The results of mud erosion test and field tests indicate that the detonation gun coated tungsten carbide coatings exhibit superior erosion resistance than all other coatings tested. The hard coatings can be applied on finished

drill bit cones and polycrystalline diamond compact bits without damaging the cutters or substrate material.

[9] **W.Tabakoff et al. (1995)** designed a high temperature erosion test facility to provide erosion data in the range of operating temperatures experienced in compressors and turbines. In addition to the high temperatures, the facility properly simulates all the erosion parameters which were determined to be important from the aerodynamics point of view. These parameters include particle velocity, angle of impact, particle size, particle concentration and sample size. Experimental study which was conducted to investigate the erosion behavior of titanium carbide coating exposed to fly ash and chromite particles. The chemical vapor deposition technique (CVD) was used to apply a ceramic coating on nickel and cobalt based superalloys (M246 and X40). The test specimens were exposed to particle laden flow at velocities of 305 and 366 m/s and temperatures of 550°C and 815<sup>0</sup>C.

[10] **P.Fauchais et al. (1996)** showed that the spray parameters affect certain factors of the coating, such as the size and distribution of porosity, oxide content, residual stresses, macro and micro cracks, factors which have an important influence on the performance and eventual failure of the coating.

[11] **Yi Maozhong et al. (1996)** evaluated the abrasability and erosion resistance of seal coatings by sliding wear and erosion. From his study he showed that the mechanism of sliding wear was ploughing accompanying with adhesive wear and oxidation wear. He showed that that the erosion resistance of the coating is mainly dependent on hardness but polyester increase the erosion resistance at high impact angle due to its cushioning effect.

[12] **Peter J Blau (1997)** summarized the research on the wear of metals which took place over the past half century and has brought new understanding and advanced major concepts of tribology. He depicted that the availability of new testing methods and instruments have made possible the detailed study of the microstructure, nanostructure, and compositions of contact surfaces. The classical work of the earlier decades concentrated on the mechanics of solid contact, understanding the true area of contact, asperity plasticity, and transfer during sliding. Wear science also witnessed the establishment of the conceptual groundwork for such things as the critical angle for maximum erosion rate by particles, the proportionality between hardness and abrasive wear rate, and the nature of slip and stick in fretting contact. Later decades brought forth instruments, like the scanning electron microscope and the atomic force microscope, which have provided fascinating insights and detailed information on surface structure. There have also been developments in computational modelling of wear by finite element methods, molecular dynamics, and fracture mechanics. Past trends in the

study of various forms of metal wear and future trends and needs in wear research were discussed.

**[13] John T Burwell (1997)** described the four principal types of mechanical wear, namely, adhesive, abrasive, corrosive and surface fatigue, as well as several minor types. Quantitative equations were derived in three cases relating the amount of wear material removed from the surfaces or their useful life to operating conditions such as distance of travel, speed, applied load and mechanical properties of the surface. These equations were compared with experiment, where such exists, and agreement was found in general to be good over certain ranges although more carefully controlled experiments are needed. Hence the relations may be used by the designer and engineer in designing and constructing equipment having moving parts in which wear will be encountered.

**[14] Erich Lugscheider et al. (1998)** described that the today's thermally sprayed MCrAlY coatings are commonly manufactured by the vacuum plasma spraying (VPS) process. This technique provides dense and oxide-free coatings. However, mainly due to the vacuum procedures this production is cost intensive and time consuming. He also described that the third generation of high-velocity oxy-fuel (HVOF) systems nowadays offer processing of materials that are sensitive to oxidation even in atmosphere. This is mainly due to the achievement of higher kinetic energy of the particulates and lower melting degrees which enables particle flattening in a plastic state. He presented a work which was focused on the influences of process parameters of a gas-driven HVOF system on the microstructure and oxygen content of MCrAlY coatings. The major parameters were subjected to DOE investigation to estimate both single and interacting effects. It was found that spray distance, fuel/oxygen ratio and powder feed rate exert a major influence on microstructure and oxygen content, whereas powder feed gas rate is not significant. Further parameters of significance were substrate temperature, shroud-gas type, fuel-gas type and powder size fraction.

**[15] I.M.hutchings et al. (1998)** outlined a simple theoretical treatment of abrasive and erosive wear tests, in which the concept of the 'tribological intensity' of the test conditions was introduced. Available test methods are reviewed and their suitability for thinly coated samples was discussed. He suggested that there is considerable scope for further development of tests since only a few were satisfactory for these important applications.

**[16] L.C.Erickson et al. (1999)** obtained a series of plasma sprayed coatings of controlled microstructure by spraying three monosize sapphire powders using an axial injection torch in which the plasma gas composition and nozzle diameter were the only processing parameters varied. The effects of changes in these parameters on the coating splat morphology, porosity,

angular crack distribution, and hardness were reported. The microstructural quality of plasma sprayed coatings and, hence, the coating properties can be improved significantly by minimizing variations in processing and raw material parameters.

**[17] Maozhong Yi et al. (1999)** investigated the friction and wear behavior of several kinds of middle temperature abradable seal coatings used in aircraft turbine engine. Their abradability was evaluated by sliding worn volume. The mechanisms of the sliding wear of the coatings were abrasive wear, adhesive wear and oxidation wear, but the weight of the adhesive wear and abrasive wear was different in different coatings and under different test loads. The results show that the abradability decreases with the increase of the hardness for a given kind of coating. Even if the hardness was close, the abradability is very different in different kinds of coatings. So, only by the hardness the level of abradability be not judged and the coating not be chosen and designed. The abradability of M313 type of coating was the best, M310 was close to M601 and M307 with low hardness was fairly good, but M307 with high hardness was the worst.

**[18] J.A.Hearley et al. (1999)** investigated the erosion behaviour of high velocity oxy-fuel thermal HVOF. NiAl intermetallic compounds coatings over a range of angles and particle velocities, in air at room temperature. Results showed a variation of mass loss with velocity and angle. Maximum erosion was observed at 90 degree for all velocities, suggestive of classical brittle behaviour. Morphological examination of the coatings' top-surface indicated that the mechanism for coating removal was in fact ductile. These apparently contradictory results were attributed to erodent characteristics, i.e., morphology, size and hardness. The erosion resistance of this coating was also compared to other thermally sprayed coatings. Results indicated that the HVOF NiAl IMC coating performed better than both metal and ceramic thermally sprayed coatings

**[19] J.A.Hearley et al.(2000)** used a high velocity, oxy-fuel (HVOF) thermal spray process to deposit two commercially available NiAl intermetallic powders, one reaction sintered and the other inert gas atomized. It was possible to deposit high quality coatings of NiAl intermetallic at rates comparable to those of non-metallic coatings. The coatings were characterized in terms of microstructure, oxygen content, porosity and permeability, Young's modulus and hardness. Coating characteristics and properties were found to be dependent on both the powder's particle size and the spray parameter's oxygen to fuel ratio.

**[20] Bu Qian Wang et al. (2002)** investigated the high velocity oxygen fuel (HVOF) sprayed chromium carbide-metal cermet coatings. This work was undertaken to understand the influence of powder type on the hot erosion behavior of HVOF coatings. A series of hot

erosion tests was carried out on eight chromium carbide-metal cermet coatings using a nozzle type elevated temperature erosion tester. The morphology of specimens was examined by light microscopy and scanning electron microscopy (SEM) with energy-dispersive spectroscopy (EDS). The composition of starting powders and deposited coatings was analyzed using EDS. It was found that among the eight HVOF chromium carbide-metal cermets coatings tested the composite powder sprayed coatings had nearly the same composition as the starting powders, while the blend powder sprayed coatings had lower chromium and higher nickel contents than the starting powders. This means that more chromium carbide particles had lost during spraying the blend powders, as compared with spraying the composite powders whose composition almost remained the same. The composite powder sprayed coatings also showed higher micro hardness and finer microstructure, lower porosity and oxide rate, which account for their higher erosion resistance than the blend powder sprayed coatings.

**[21] M.P.Planche et al. (2002)** studied the effect of the oxygen fuel ratio on the particle characteristics during their flight in the jet. A comparison between the oxide contents in Inconel 718 coatings was established as a function of the spray parameters. Electrochemical measurements were performed, giving information on the role of the oxides present in the coating in relation to its corrosion behavior. Finally, directions were proposed to optimize coating properties obtained with the HVOF process in relation to the in-flight particle characteristics.

**[22] Lima et al. (2003)** presented a work in study and characterization of tungsten and chrome carbides based coatings. The coatings were applied by high velocity oxy fuel thermal spraying (HVOF), using two different HVOF systems. Microstructure, hardness, as well as wear characteristics of the coatings were evaluated. The results showed that the obtained coatings present great characteristics and can successfully faces several wear conditions.

**[23] Lidong Zhao et al. (2004)** sprayed WC-CoCr powder using a HVOF process. The spray parameters were varied to study their influence on the particle in-flight properties and the coating properties using on-line particle monitoring. The wear behavior of the coatings was evaluated both by rubber wheel tests and by pin-on-disk tests. It was found that the total gas flow rate and the powder feed rate could strongly influence the particle in-flight properties under the spray conditions in the study. By contrast, the spray distance had less influence than the above two parameters. In general, the higher the total gas flow rate, the lower the powder feed rate and the shorter the spray distance, the higher the particle velocity and

temperature, and the denser and harder the coating. The rubber wheel tests showed that the total gas flow rate was of large significance for the wear resistance of the coatings.

[24] **T.S.Sidhu et al. (2005)** investigated that materials operating at high temperatures in corrosive media suffer erosion-corrosion wear, oxidation, and hot corrosion. Among various methods used for the protection of the surfaces against degradation, we can especially mention the technology of application of coatings by high-velocity oxy-fuel spraying, which gives coatings which high strength and hardness, low (less than 1%) porosity, and high erosion-corrosion and wear resistances. The characteristics of the coatings and their protective properties were presented. The role of some high-velocity oxy-fuel coatings in the protection of metals and alloys against degradation at high temperatures in various media was demonstrated.

[25] **H.I.Faraoun et al. (2006)** characterized the microstructure of recently developed abradable materials for providing a sealing between rotating and stationary parts in aerospace turbine engines. The investigated materials were two coatings obtained by thermal spraying of composite powder particles from the AlSi-hBN and NiCrAl-bentonite systems. X-ray diffraction and scanning electron microscopy were used to analyse the microstructure and identify the structural elements of the coatings. These structural elements: the coarse porosities, the metallic binding phase and the embedded “abradable” particles were analysed by quantitative metallography.

[26] **Xiao Ma et al. (2007)** analyzed three proprietary plasma-sprayed coatings, Ni-graphite, Al-Si-graphite and Al-Si-polyester. The scratch test behaviour was correlated with the mechanical properties of each coating (elastic modulus, microhardness and UTS (ultimate tensile strength)). Results were compared with those from industrial trials, to ascertain if the scratch test could be used as a relatively cheap and effective alternative to expensive engine trials. He showed that the “Progressive abrasability hardness”(PAH) can be utilised as a measure of abrasability in the scratch test, and can be related to the mechanical properties, in a manner consistent with engine test-bed findings..

[27] **M.Gaona et al. (2008)** deposited nanostructured titania feedstock via high velocity oxy-fuel (HVOF) spraying onto Ti-6Al-4V substrates. Using in-flight particle diagnostics, different particle temperatures and velocities were employed in order to reveal their effects on microstructure and mechanical properties of the coatings. A series of linear dependencies were observed involving processing conditions (i.e., in-flight particle temperature and velocity) and characteristics of the resulting coating micro structural features and properties, such as, phase composition,

[28] **M.Hasan et al. (2008)** predicted that the High Velocity Oxy–Fuel (HVOF) process is one of the most versatile thermal spray technologies and has found use in many industries due to its flexibility and cost effectiveness. He showed that the gradual changes of microstructure in functionally graded coatings reduce possible residual stress build-up by gradually attaining property changes between the substrate and the coating. He investigated the effect of spray parameters on residual stress build-up in aluminium/tool-steel functionally graded coatings (FGC). He used simple  $3^3$  factorial design of experiments to establish the effects of spray parameters on residual stress. Parameters such as flow rate ratio of the oxygen to propylene, flow rate of the compressed air and spray distance were varied during coating deposition. Apart from the thickness of the coated sample, the spray distance showed greater effect on residual stress build-up in the graded coatings compared to flow rate ratio of the oxygen to propylene, and flow rate of the compressed air. Finally a set of values of spray parameters giving the best compromise between low residual stress and high deposited coating thickness were identified.

[29] **Adnan Al-Bashir et al. (2009)** studied that there are several factors to be controlled in HVOF process, this makes it necessary to get the best combination of process parameters to provide the required level of wear resistance and, hence part life. In his study he applied oxy-fuel process to 4140 alloy steel. Process parameters used were acetylene gas pressure, stand-off distance and rotational speed had been varied using a  $2^k$  experimental design. The Pin-on-Disc test was used to estimate the wear resistance of the different material-coating-parameters combinations. The data were analyzed and a statistical model, explaining the effect(s) of different parameters as well as their interaction.

[30] **S.S.Mahapatra et al. (2009)** investigated the erosion wear response of composites and presents a comparison on the influence of three different particulate fillers cement by-pass dust (CBPD), alumina ( $Al_2O_3$ ) and silicon carbide (SiC) on the wear characteristics of glass–polyester composites. For this purpose, the erosion test schedule in an air jet type test rig was made following design of experiments approach using Taguchi’s orthogonal arrays. Taguchi approach enables to determine optimal parameter settings that lead to minimization of erosion rate. The results indicate that erodent size, filler content, impingement angle and impact velocity influence the wear rate significantly.

[31] **D.P.Kashyap et al. (2010)** explained that high velocity oxy-fuel (HVOF) spraying process is a new and rapidly developing technology, which can yield high density coatings with porosity less than 1%, having high hardness and adhesion values, and good erosion, corrosion and wear resistance properties. The quality of coating is directly related to the

spraying parameters such as spray distance or stand of distance, powder feed rate, carrier gas feed rate, oxygen-fuel ratio, substrate temperature, shroud-gas type, powder size fraction, in-flight temperature of powder particle. Effects of various parameters of HVOF process on the erosion-corrosion and behavior of the coatings were reviewed.

[32] **Christophe Lyphout et al. (2010)** found that fundamental understanding of relationships between process parameters, particle in-flight characteristics, and adhesion strength of HVOF sprayed coatings is important to achieve the high coating adhesion that is needed in aeronautic repair applications. In his study, he used statistical Design of Experiments (DOE) to identify the most important process parameters that influence adhesion strength of IN718 coatings sprayed on IN718 substrates. Special attention was given to the parameters combustion ratio, total gas mass flow, stand-off distance and external cooling, since these parameters were assumed to have a significant influence on particle temperature and velocity. He found that higher the particle velocity and the particle temperature, the higher the adhesion strength. He derived a clear relationship between particle in-flight properties and coating microstructure that the higher the particle velocity, the lower the porosity level and higher the oxides content.

[33] **Maria Oksa et al. (2011)** reviewed High Velocity Oxy-fuel (HVOF) thermal spray techniques, spraying process optimization, and characterization. Different variants of the technology were described and the main differences in spray conditions in terms of particle kinetics and thermal energy were rationalized. Methods and tools for controlling the spray process were presented as well as their use in optimizing the coating process. It will be shown how the differences from the starting powder to the final coating formation affect the coating microstructure and performance. It was emphasized that optimization of the spraying process is a must.

[34] **Y.Wang et al. (2012)** prepared a FeCrMoMnWBCSi amorphous metallic coating by using high velocity oxy-fuel spray. The influence of processing parameters on coatings microstructure, porosity level, amorphous phase fraction and corrosion behaviour of the coatings was characterized by scanning electron microscopy, X-ray diffraction, differential scanning calorimeter and electro-chemical methods. The results indicated that the microstructures of the coatings were sensitive to the spray parameters considerably. Porosity and unmelted particle proportion decreased with the oxygen/fuel (O/F) ratio and increased with the powder feed rate. The trend of oxides content was opposite to the porosity and unmelted particle proportion. The coatings obtained with higher O/F ratio and lower powder feed rate exhibited higher hardness.

[35] **Houdkova et al. (2012)** described the methodology of parameters optimization process in HVOF sprayed STELLITE 6 coating with the results of coating properties evaluation. Based on the results, the best spraying parameters were found to be used for further spraying of STELLITE 6 for commercial applications and to preserve its superior properties.

[36] **Yi Maozhong et al. (2012)** investigated the erosion wear behaviour of abradable coatings in a self made CMS-100 vacuum sand erosion machine. He showed that the relationship between the erosion mass loss and erosion time is linear, the coating hold maximum erosion rate at  $60^{\circ}$  impact angle and the relationship between the erosion rate and impact speed is an exponential function.

[37] **A.J.Lopez et al. (2013)** used High velocity oxygen-fuel (HVOF) as fabrication technique to deposit aluminium coatings reinforced with silicon carbide particles on Mg–Zn substrates. The aim of the investigation was to improve the tribological performance of the ZE41A magnesium alloy. The parameters of the thermal spraying system have been optimized in order to maximize the SiC particles incorporation in the aluminium matrix of the coating and to minimize the mechanical deterioration of the light alloy substrate. The wear resistance of the substrates was increased and the wear rate decreased in two orders of magnitude respect to that of the bare Mg-alloy after the optimization of the spraying parameters.

[38] **D.Sudhakra et al. (2013)** used Taguchi method for optimization of Wire electric discharge machining (WEDM) process parameters with response cutting rate(material removal rate).Optimum levels of parameters were found using taguchi method and significant parameters were determined by ANOVA.

**3.1 GAPS IN LITERATURE**

From the literature study of abrasible coatings it is found that previous researches focused only to the study of powders, spray processes, properties of the coating and the relationship among them. But, the basic researches about the abrasibility and erosion resistance have not been well-made. The coating properties are influenced not only by the properties of the used powders but also significantly by the used spray process and spray parameters.

Plasma spraying mostly used to deposit abrasible coatings on the surface of alloys. In plasma spraying the kinetic energy of the sprayed particles is low and their thermal energy is high. This causes the appearance of some defects in the coatings such as pores, cracks or irregularities in phase distribution as well as oxide inclusions. These defects significantly influence the properties of the coating. High Velocity Oxygen Fuel (HVOF) sprayed coatings are attractive because they are dense and exhibit low oxidation of raw materials compared to coatings obtained by other thermal spray processes (plasma or wire arc spray). Cost effectiveness of HVOF spraying is also a significant factor.

**3.2 PROBLEM FORMULATION AND RESEARCH OBJECTIVE**

The present study will aim to improve the erosion resistance and abrasibility of the HVOF sprayed abrasible coating. Taguchi design of experiments technique shall be used for determining effects of spraying parameters on erosion resistance and hardness.

The objective of this study focuses on the development of thick coating (350 $\mu$ m) of AlSi-Polyester (Abradable) on SuperCo-188(cobalt based alloy) using the HVOF spray process. Studies on erosion resistance and hardness of coated substrates were carried out using an erosion wear test rig and Rockwell Hardness tester (Y-scale). Taguchi's DOE (Design of Experiments) will be applied for analyzing the results and finding the best combinations of parameter settings that give best results.

**4.1 DESIGN OF EXPERIMENT**

The quality engineering methods of Dr. Taguchi, employing design of experiments (DOE), is one of the most important statistical tools of TQM for designing high quality systems at reduced cost. Taguchi methods provide an efficient and systematic way to optimize designs for performance, quality, and cost. Fundamentally, traditional experimental design procedures are too complicated and not easy to use. A large number of experimental works have to be carried out when the number of the process parameters increases. Taguchi method uses a special design of orthogonal arrays to study the entire parameter space with only a small number of experiments. Taguchi methods has been widely utilized in engineering analysis and consists of a plan of experiments with the objective of acquiring data in a controlled way and in order to obtain information about the behaviour of a given process. The greatest advantage of this method is to save the effort in conducting experiments. Therefore, it reduces the experimental time as well as the cost by finding out significant factors fast.

In the present study the effect of spraying parameters in HVOF i.e. oxygen flow rate, fuel flow rate (propylene) and spray angle were studied using parameterization approach developed by Taguchi.

**4.2 STEPS APPLIED IN DESIGN OF EXPERIMENTS**

Taguchi proposed a standard procedure for applying his method for optimizing any process. The steps applied are as follows:

**4.2.1) Determine the quality characteristic to be optimized**

The first step in the Taguchi method is to determine the quality characteristic to be optimized. In the present study our aim is to evaluate the main effects of HVOF spraying parameters on mechanical and physical properties such as erosion rate, and hardness of coating.

**4.2.2) Identify the control parameters and their alternative levels**

The next step to identify the control parameters thought to have significant effects on the quality characteristic. In the present study oxygen flow rate, fuel flow rate, spray angle were control (test) parameters or design factors that can be set and maintained. 3 levels (test values) for each test parameter were chosen. Test parameters and their respective levels are shown in table 4.1

Table 4.1 Process Parameters and Their Levels

Sr.No.	Parameters	LEVEL 1	LEVEL 2	LEVEL 3	UNITS
1	O <sub>2</sub> flow rate (OF)	300	350	400	L/min
2	Fuel flow rate (FF)	55	65	75	L/min
3	Spray angle (SA)	60	75	90	degree

#### 4.2.3) Design the matrix experiment and define the data analysis procedure

The next step was to design the matrix experiment and define the data analysis procedure. First, the appropriate orthogonal arrays for the noise and control parameters to fit a specific study are selected. In the present study L-9 orthogonal array was selected. Three levels were used for each factor as shown in Table 4.1, yielding nine different experimental combinations and thus prepared total of 9 samples with different spray parameters as shown in Table 4.2

Table 4.2 Orthogonal Array

Sample No.	Oxygen Flow (OF) (L/min)	Fuel Flow (OF) (L/min)	Spray Angle (SA) (degree)
1	300	55	60
2	300	65	75
3	300	75	90
4	350	55	75
5	350	65	90
6	350	75	60
7	400	55	90
8	400	65	60
9	400	75	75

#### 4.3 SUBSTRATE MATERIAL:

In the present study SuperCo-188(Cobalt based superalloy) used as a substrate material. SuperCo-188 is a cobalt-nickel-chromium-tungsten superalloy that combines excellent high-temperature strength with very good resistance to oxidizing environments up to 1095°C for prolonged expo-

tures, and excellent resistance to sulfate deposit hot corrosion. SuperCo-188 combines properties which make it suitable for a variety of fabricated component applications in the aerospace industry. It is widely used in established military and commercial gas turbine engines for combustion cans, transition ducts, and after-burner components. By using a diamond cutter samples of size 24mmx18mm cross sectional area and 5 mm thickness were cut. In the present work, the specimens as the substrate material were purchased from MIDHANI (Mishra Dhatu Nigam) Limited located in Hyderabad, India. MIDHANI was established in 1973 and is the prime manufacturers of Super alloys.

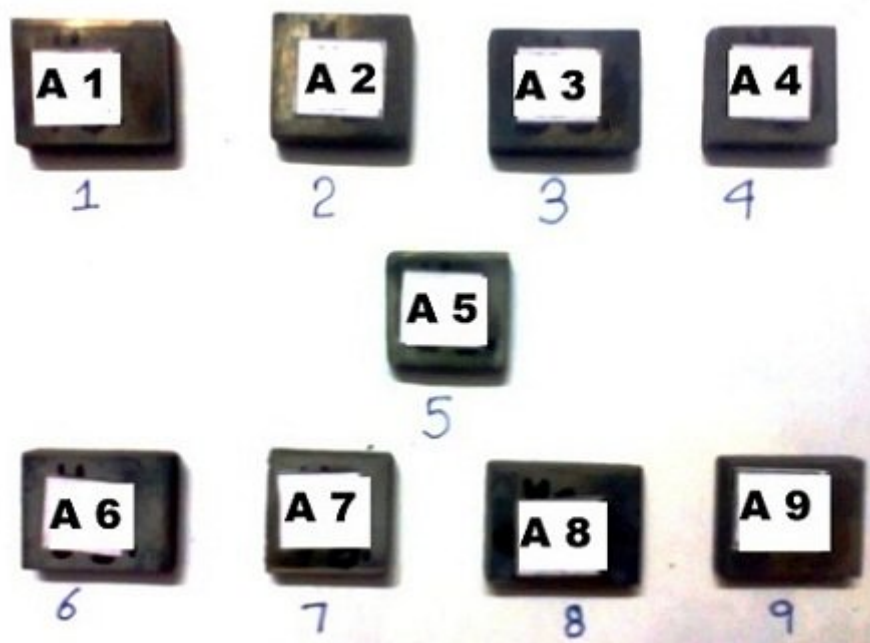


Figure 4.1 Photograph of Substrate (uncoated)

#### 4.4 PROPERTIES OF SUBSTRATE MATERIAL

The various properties of substrate material have been discussed below:

##### 4.4.1) Chemical Composition:

Table 4.3 Chemical Composition of SuperCo-188

Component	Co	Ni	Cr	W	Fe	Mn	Si	C	La	B
Percentage Composition	Balance	22.0	22.0	14.0	3.0	1.25	0.35	0.10	0.03	0.015

#### 4.4.2) Microhardness:

Microhardness of substrate material (uncoated) was determined by using micro hardness tester (as shown in figure 4.2). A load of 500gm was applied by using a calibration distance of 25 units. Vickers hardness number (VHN) for substrate was determined. During the application of load dwell time was 20 seconds.



Figure 4.2 Microhardness Tester



Figure 4.3 Indent on Specimen

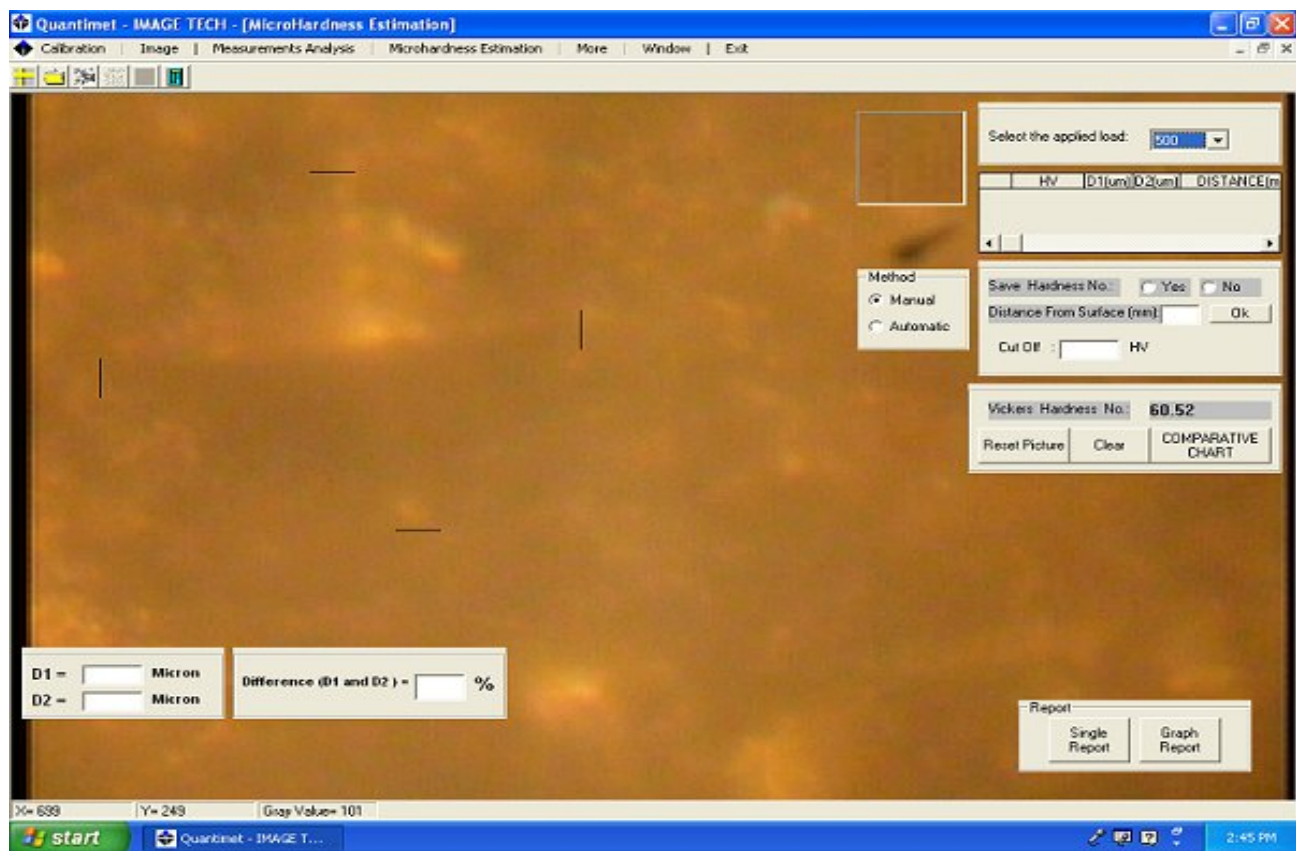


Figure 4.4 Vickers Hardness Number of Specimen (uncoated)

Table 4.4 Specimens Microhardness

Sr.No.	Hardness(HV) (Test-1)	Hardness(HV) (Test-2)	Hardness(HV) (Test-3)
1	59.92	60.30	60.52

#### 4.5 STEPS FOLLOWED FOR SAMPLES PREPARATION

These steps involved surface preparation of substrate material and include a series of physical and/or chemical pretreatments to enhance the adhesive strength of a surface to be coated.

1. First of all acid pickling is done for the removal of grease and oil from a surface by immersing the substrate in liquid organic solvents.
2. Shot Peening on the surface of substrate is done to induce compressive stresses.
3. The substrate material was rinsed in acetone and cleaned with emery paper.
4. Samples were dried properly.
5. Using a diamond cutter samples of required dimensions were cut.
6. Coating of the samples was done as per requirement by setting the parameters on machine.

Size of samples prepared were **24mm x 18 mm x 6mm**

#### 4.6 COATING

In the present study Cobalt based superalloy (SuperCo-188) coated with AlSi-Polyester powder commercially available as METCO 601NS abrasible powder using High Velocity Oxy Fuel (HVOF) method. The substrate material is coated at Metallizing Equipment Company Pvt. Ltd. Jodhpur (Rajasthan) which was established in 1967 and is the prime supplier of HVOF coating, internal spray gun, blasting machine, metal spray coating, boiler tube coating etc.

In this coating process, the fuel (Gas/Liquid) along with oxygen is introduced into the combustion chamber where it burnt and high temperature pressure combustion products exhausted through nozzle. The powder to be coated is supplied along with this superheated high velocity stream. The powder, in this superheated high velocity stream get melted and deposited on sample surface. In this coating process PROPYLENE was used as fuel (Gas) and nitrogen gas was used as a carrier gas to circulate/supply the powder along with superheated, high velocity stream. Figure 4.5 showing the HVOF coating machine situated at Metalizing Equipment Company Pvt. Ltd, Jodhpur.

The indicator (in figure 4.5) in the control panel indicates the flow of fuel gas, oxygen gas and

carrier gas. The powder was filled in the black box just below the indicators.



Figure 4.5 High Velocity Oxy-Fuel (HVOF) Coating Machine.

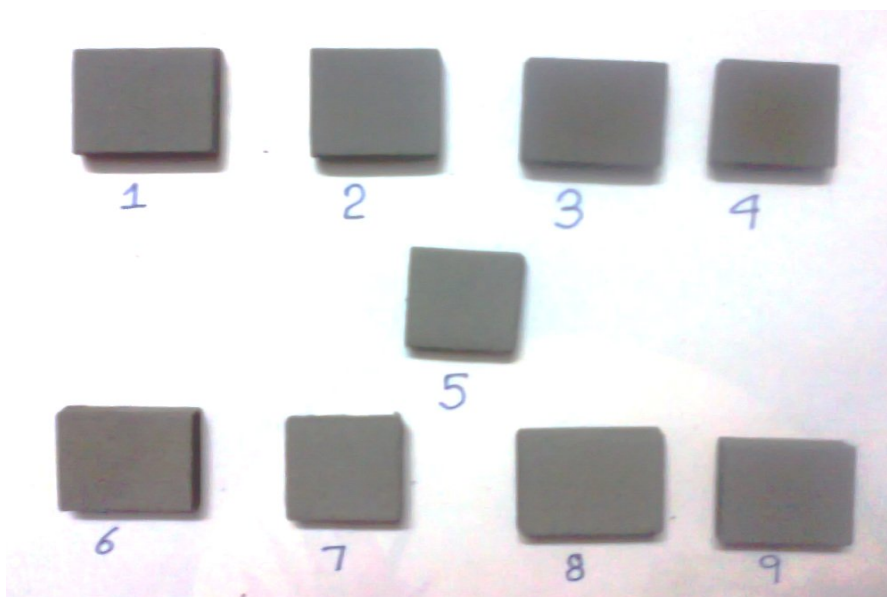


Figure 4.6 Photograph of Coated Samples

#### 4.7 COATING POWDER

In the present work SuperCo-188 which is used as substrate metal is coated with the abradable material (METCO 601NS) which is composed of the aluminium (Al), Silicon (Si) and the polyester. Aluminum Silicon – Polymer powders produce abradable coatings for clearance control applications where the rotating component may come into contact with the coating as a result of design intent or operational surges. The coatings are designed to minimize the wear to the rotating components while maximizing gas path efficiency by providing clearance control in seal areas. These powders produce abradable coatings with excellent rub characteristics. They provide the optimum balance between the desired properties of abradability, erosion resistance and hardness. Metco 601 NS has an exemplary service reputation, with many thousands of engine components having been coated with this material.

Table 4.5 Properties of METCO 601NS

Composition(weight percent)	Aluminium=53, Silicon=7, Polyster=40
Shape	Rounded, irregular
Particle Size( $\mu\text{m}$ )	-125+11
Maximum Service Temperature( $^{\circ}\text{C}$ )	325
Coating Density( $\text{g}/\text{cm}^3$ )	1.55
Microhardness(HR15Y)	70
Deposition Efficiency	$\leq 65\%$
Thermal Conductivity(W/mK)	0.53
Melting Point	$577^{\circ}\text{C}$
Bond Strength	9.7 MPa
Manufacture Method	Blended
Coating Thickness	$350 \pm 10$
Chemistry	Al-Si polymer

The microstructure of the AlSi-Polyester abradable coating is a continuous matrix of aluminum with fairly well dispersed particles of polyester. The aluminum provides good bond strength, good inter-particle strength and good thermal properties. The polyester provides abradability and a low coefficient of friction.

## 4.8 TESTS CONDUCTED

### 4.8.1) Erosion Test:

Erosion wear test of abradable coating of METCO 601 NS were performed on a jet erosion tester situated at University Institute of Engineering & Technology (UIET) Kurukshetra, Haryana. Silica sand and compressed air mixture is used as slurry medium.

The erosion wear test rig consists of various components like air compressor, copper tube, air heating coil, temperature sensor, industrial oven (furnace), feed control valves, hopper containing sand, heat control valves, work piece holder with angle adjusting screw and nozzle etc. The erosion wear test apparatus is shown in figure 4.7:

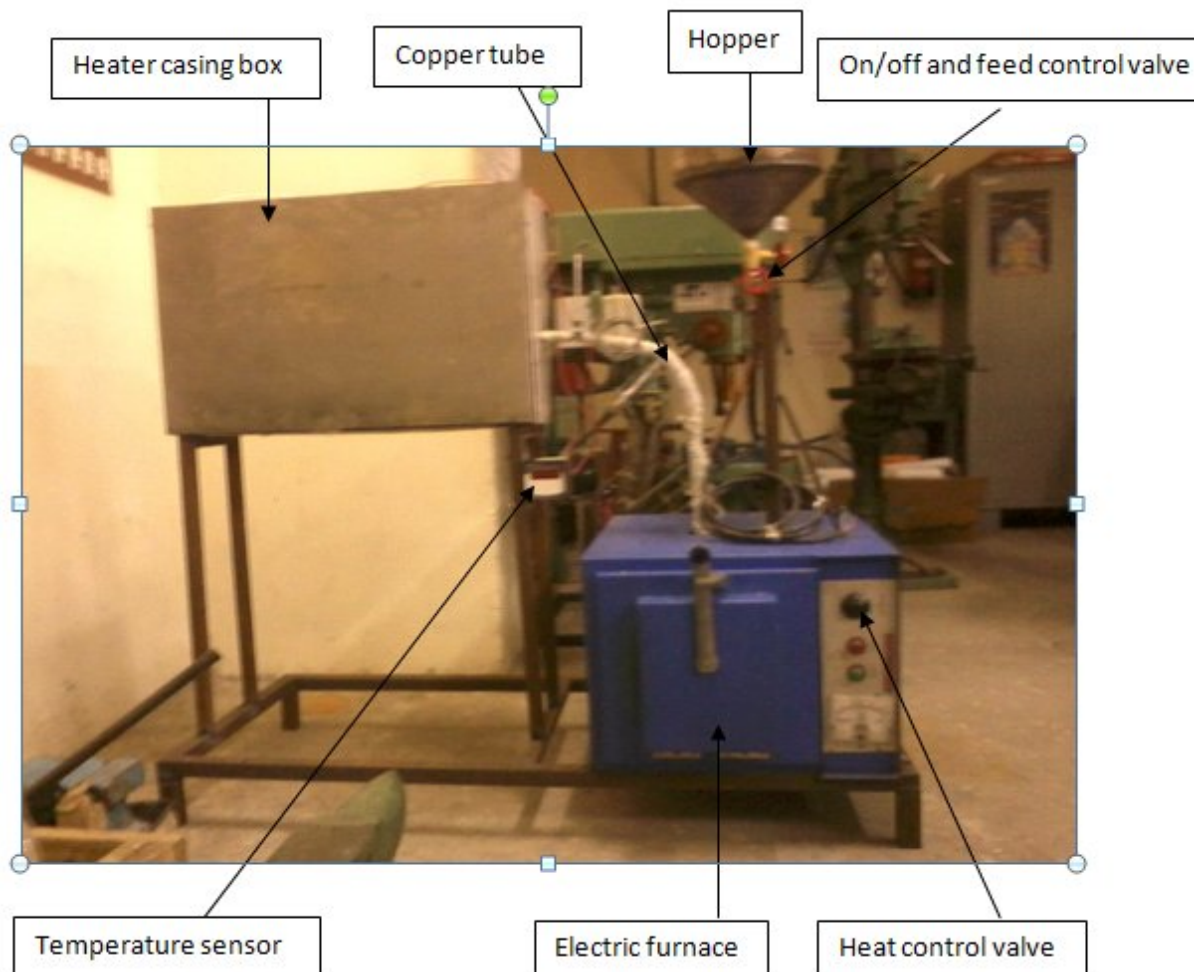


Figure 4.7 Erosion testing apparatus

In air jet erosion testing a high velocity jet strikes a flat specimen at some adjustable angle. In this test, the amount of material removed is determined by the weight loss. The weight loss of the

specimen corresponds to the average erosion over the surface. Jet erosion tester has been developed to investigate the effect of different parameters.

Table 4.6 Control Parameters of Erosion Testing Apparatus

Sr. NO.	Description	Parameter Range
1.	Impingement angle	5 <sup>0</sup> to 90 <sup>0</sup>
2.	Standoff Distance	100 to 250mm
3.	Air velocity	Up to 100m/s
4.	Particle velocity	Up to 30m/s
5.	Sand Particle feed rate	5 to 15gm/ min
6.	Specimen size	24mm*18mm*5mm
7.	Nozzle Diameter	3mm
8.	Industrial Furnace	10kW
9.	Heater	1kW
10.	Air Temperature	25 to 400 <sup>0</sup> C

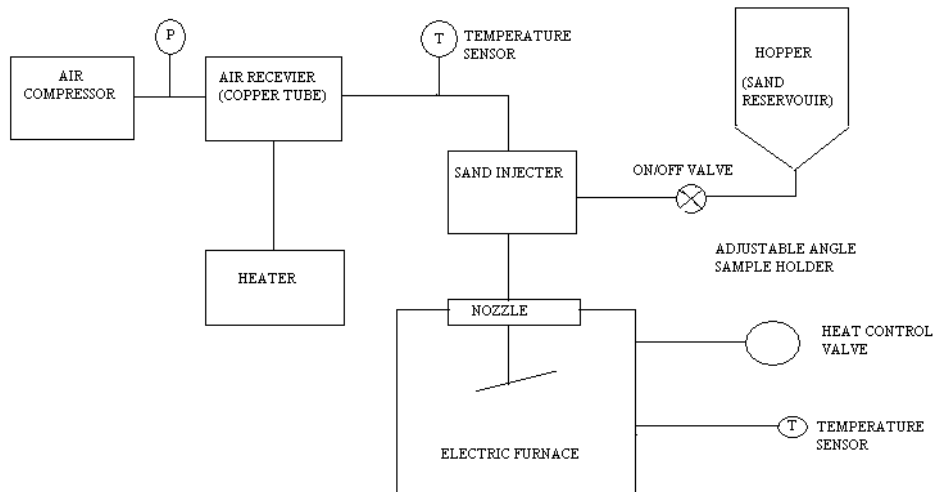


Figure 4.8 Schematics of Erosion Testing Apparatus

#### 4.8.2) Parts of Erosion Testing Machine

In this work, a high temperature erosion testing machine is used which can perform erosion test on metal substrates with coating is carried out at different impingement angles ranging from 5<sup>0</sup> to 90<sup>0</sup>.

Dry sand particles of different average sizes are used as erodent. The machine is as per ASTM G76 standards. Description of the parts of the testing machine is given below:

Table 4.7 Erosion Testing Machine Parts

S.No.	Component name	Description
1	Air compressor	A reciprocating air compressor of high pressure. Air is supplied from the reciprocating air compressor, present beside the erosion testing machine. It is a two cylinder compressor; the bigger cylinder contains air of low pressure and high volume. The smaller cylinder contains high pressured air.
2	Copper tube pipe	Copper tubes are used for conducting the compressed air into the apparatus. The copper tube diameter taken as 1.2 cm. A heater wire is wound around the copper tube for increasing the temperature of air.
3	Heater	Heater of 1000 W capacity is used for heating the air. The heater wire is wound around the copper tube for heating.
4	Heater casing box	The heater wires which are wound around the copper tube are enclosed in a casing box for heat reduction in outside environment
5	Temperature sensor	A temperature sensor which measures the temperature of air can be used. It is placed after the heating assembly and gives the temperature of air.
6	Hopper	A hopper is acts as a reservoir for storing the sand or abrasive particle. We can use hopper of 3 kg sand storage capacity. Hopper is made of iron material.
7	Feed rate control valve	A feed rate control valve control the supply of sand particle and maintain the feed rate of sand.

<b>S.No.</b>	<b>Component name</b>	<b>Description</b>
8	Substrate holder	A fixture is provided to hold the sample or specimen at different angles to the nozzle. The fixture arrangement has one metal plate which moves over a gradually marked arrangement. The fixture can be arranged at different angles
9	Nozzle	The nozzle is connected with the copper tube through which mixture of pressured air and sand particle enters the nozzle mouth.
10	Electric furnace	Electric furnace is a standard box of internal dimension length 360mm, breadth 125mm, height 175mm. Capacity or power of electric furnace is 10KW. Furnace has heater wire inside so that the temperature inside is very high. Fixture arrangement assembly is taken in the electric furnace.

Erosion wear experiments that we have performed in this erosion testing machine are done through a sequence of steps, in which most of the observations recorded manually. The mass loss of the specimen after each test is the measure of erosion wear. The sequence of steps of experimental procedure is as given below:

- 1) Before conducting the test the specimen surface was cleaned properly.
- 2) Weighing the specimen (initial weight).
- 3) The sample is clamped at the fixture. The required angle and standoff distance was adjusted
- 4) The air at required pressure is mixed with the erosive particle and is directed towards the specimen for specified time duration.
- 5) Perform the test as per set values (flow rate, impact angle and required time interval).
- 6) Unclamp the specimen from specimen holder
- 7) Weighing the specimen after erosion to measure the mass loss
- 8) For further observations repeat the procedure steps as per requirement.

### 4.8.3) Experimentation Parameters

Values of parameters for experimentation were chosen from the study of the previous researchers and literature. The parameters and their values selected for experimentation were those which give maximum erosion rate.

Table 4.8 Experimentation Parameters:

Dimensions of Specimen	24 mm × 18 mm × 5 mm
Angle	60°
Sand particle feed rate	20 gm/min
Sand particle Size	100-200 micron
Stand Off Distance	100 mm
Time	Maximum 2 hours
Air Velocity	80 m/s
Substrate temperature	300°C

### 4.9 ROCKWELL SUPERFICIAL HARDNESS TEST (Y-SCALE)

The Rockwell Superficial hardness test method consists of indenting the test material with a diamond cone or hardened steel ball indenter. The indenter is forced into the test material under a preliminary minor load  $F_0$  (Fig. 4.9A) usually 3 kgf. When equilibrium has been reached, an indicating device that follows the movements of the indenter and so responds to changes in depth of penetration of the indenter is set to a datum position. While the preliminary minor load is still applied an additional major load, is applied with resulting increase in penetration (Fig. 4.9B). When equilibrium has again been reach, the additional major load is removed but the preliminary minor load is still maintained. Removal of the additional major load allows a partial recovery, so reducing the depth of penetration (Fig. 4.9C). The permanent increase in depth of penetration,  $e$ , resulting from the application and

removal of the additional major load is used to calculate the Rockwell Superficial hardness number.

i.e.  $HR = E - e$

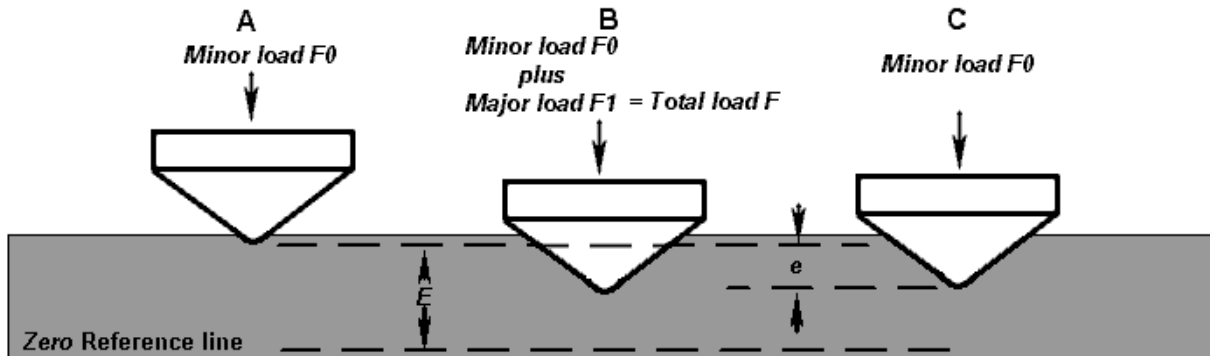


Fig. 4.9 Rockwell Superficial Principle

#### 4.9.1) Rockwell Superficial Hardness Scales

Table 4.9 Rockwell Superficial Hardness Scale

Scale	Indenter Type	Minor Load $F_0$ kgf	Major Load $F_1$ kgf	Total Load $F$ kgf	Field of Application
HR 15 W	1/8" steel ball	3	12	15	For metals with very low hardness and for very thin cases, for example thin linings of antifriction metals, HRX and HRY especially for sintered metals
HR 30 W	1/8" steel ball	3	27	30	
HR 45 W	1/8" steel ball	3	42	45	
HR 15 X	1/4" steel ball	3	12	15	
HR 30 X	1/4" steel ball	3	27	30	
HR 45 X	1/4" steel ball	3	42	45	
HR 15 Y	1/2" steel ball	3	12	15	
HR 30 Y	1/2" steel ball	3	27	30	
HR 45 Y	1/2" steel ball	3	42	45	

#### 4.10 ERODANT

Silica sand is used as an erodent in erosion wear testing rig. Silica sand is the most common variety of sand found in the world. Main constituent of silica sand is Silicon dioxide ( $SiO_2$ ).

Silica sand is mostly used in polishing and surfacing of glass material and sand blasting.

Spray parameters investigated in this study include oxygen flow rate (OF), fuel gas (propylene gas) flow rate (FF), spray angle (SA) during the coating process. Three levels were used for each factor.

### 5.1 ANALYSIS OF EROSION BEHAVIOR

The effects of control parameters i.e. Oxygen flow rate (OF), fuel flow rate (FF) and Spray angle (SA) on erosion rate were evaluated. Three repetitions for each of 9 runs were completed to calculate the erosion rate. The erosion rates of the specimens in milligram (mg) per kg of erodent flow were evaluated based on initial weight and final weight after subjecting the samples to erosion in an erosion wear test rig. Mass loss was measured by a sensitive balance.

Table 5.1 Result of Erosion rates with 3 trials for each

Expt. No.	Oxygen Flow (OF) (L/min)	Fuel Flow (FF) (L/min)	Spray Angle (SA) (degree)	Erosion Rate (mg/Kg)		
				Test-1	Test-2	Test-3
1	300	55	60	15.59	15.09	15.34
2	300	65	75	17.89	17.44	17.665
3	300	75	90	20.23	19.73	19.98
4	350	55	75	17.65	17.15	17.4
5	350	65	90	19.87	20.0	19.935
6	350	75	60	20.12	19.62	19.87
7	400	55	90	19.23	19.3	19.265
8	400	65	60	20.05	19.55	19.8
9	400	75	75	22.0	21.8	21.9

## 5.2 CALCULATION OF SIGNAL TO NOISE RATIO FOR RESPONSE FACTORS

S/N ratio is a response which consolidates repetitions and the effect of noise levels into one data point. Analysis of variance of the S/N ratio is performed to identify the statistically significant parameters. The analysis of the experimental data were carried out using MINITAB 15 software, which is specially used for DOE applications. The experimental results were transformed into signal-to-noise (S/N) ratios. S/N ratio is defined as the ratio of the mean of the signal to the standard deviation of the noise. The S/N ratio indicates the degree of the predictable performance of a product or process in the presence of noise factors. The S/N ratio for erosion rate is of “Smaller the better” characteristic which can be calculated as logarithmic transformation of the loss function.

$$S/N = -10\log \{ \Sigma (Y^2)/n \}$$

Table 5.2 Calculation of S/N ratio for Response factors (MINITAB Output)

Experiment No.	Oxygen Flow (OF) (L/min)	Fuel Flow (FF) (L/min)	Spray Angle (SA) (degree)	S/N Ratio	Mean
1	300	55	60	-23.7173	15.340
2	300	65	75	-24.9427	17.665
3	300	75	90	-26.0124	19.980
4	350	55	75	-24.8116	17.400
5	350	65	90	-25.9924	19.935
6	350	75	60	-25.9644	19.870
7	400	55	90	-25.6954	19.265
8	400	65	60	-25.9338	19.800
9	400	75	75	-26.8089	21.900

### 5.3 ANALYSIS OF EROSION FOR SPRAY PARAMETERS:

#### 5.3.1) Effect of input factors on erosion

The S/N ratio for each level of spray parameters are summarized and referred to the average effects in response table of mean and S/N ratio. For erosion the calculation of S/N ratio follows “smaller the better” model.

Table 5.3 Response table for S/N ratio (MINITAB output)

Level	OF	FF	SA
1	-24.89	-24.74	-25.21
2	-25.59	-25.62	-25.52
3	-26.15	-26.26	-25.90
Delta	1.26	1.52	0.69
Rank	2	1	3

Table 5.4 Response table for Mean (MINITAB Output)

Level	OF	FF	SA
1	17.66	17.33	18.34
2	19.07	19.13	18.99
3	20.32	20.58	19.73
Delta	2.66	3.25	1.39
Rank	2	1	3

#### 5.3.2) Analysis of variance (ANOVA) for erosion

The purpose of analysis of variance (ANOVA) is to determine which spray parameter significantly affects the erosion rate. Table 5.5 the result of ANOVA analysis of signal to noise data. It is apparent that the P values of all the three parameters oxygen flow rate (OF), fuel flow rate (FF), and spray angle (SA) was less than  $P = 0.05$ , thus all the three factors mentioned above affect erosion rate significantly. The most significant factor is fuel (propylene) flow rate (FF) for erosion wear response. The percentage contribution of each factor is shown in table 5.5

Table 5.5 ANOVA for S/N Ratio (MINITAB output)

Source	Degree of Freedom	Seq SS	Adj SS	Adj MS	F	P	Percentage contribution
OF	2	2.37353	2.37353	1.18676	241.89	0.004	35.92
FF	2	3.49726	3.49726	1.74863	356.41	0.003	52.93
SA	2	0.72628	0.72628	0.3614	74.02	0.013	11.00
Residual Error	2	0.00981	0.00981	0.00491			
Total	8	6.60688					

Table 5.6 ANOVA for Mean (MINITAB output)

Source	DF	Seq SS	Adj SS	Adj MS	F	P
OF	2	10.6252	10.6252	5.31258	335.47	0.003
FF	2	15.8882	15.8882	7.94409	501.64	0.002
SA	2	2.9019	2.9019	1.45095	91.62	0.011
Residual Error	2	0.0317	0.0317	0.01584		
Total	8	29.4469				

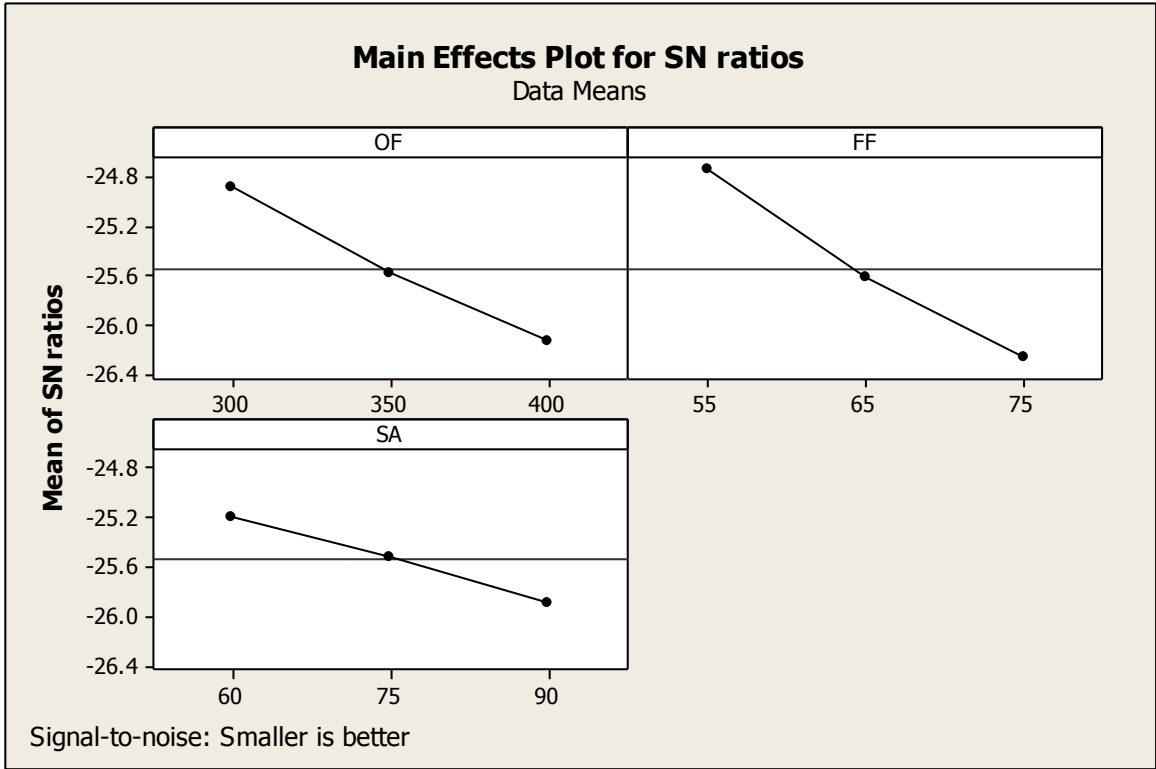


Figure 5.1 Main Effects plot for S/N Ratio

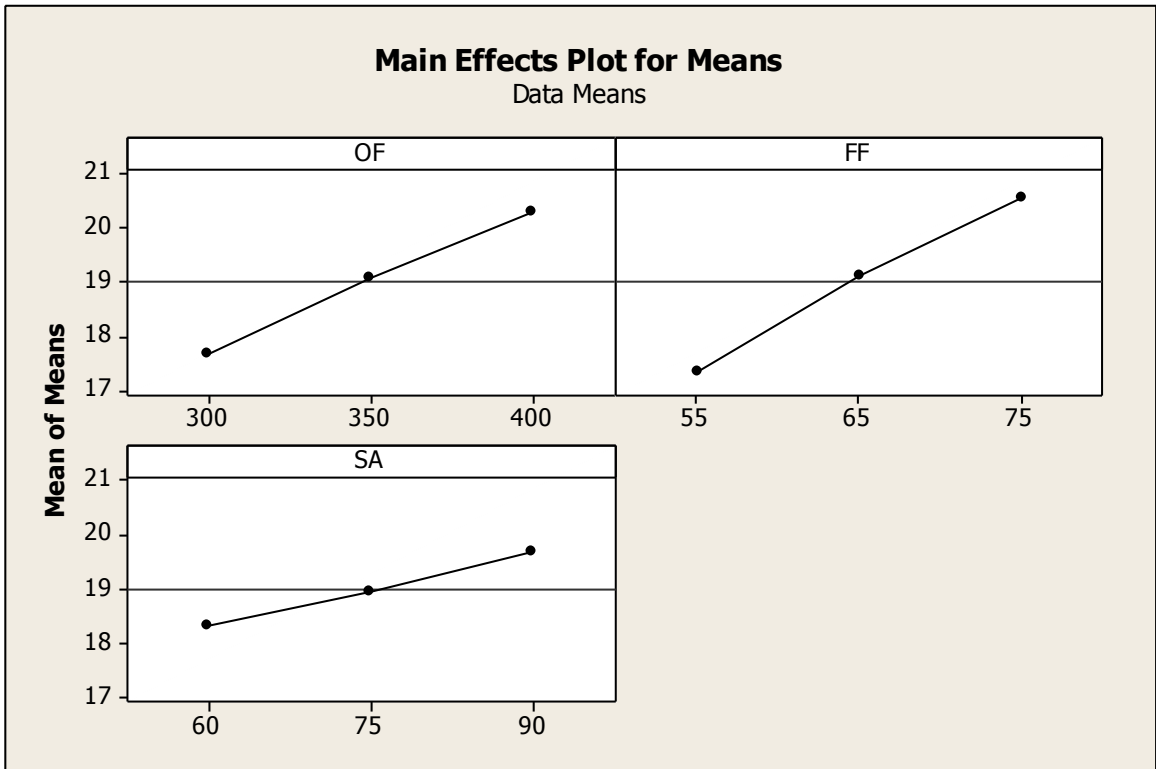


Figure 5.2 Main Effects plot for Data Means

The least variation and the optimal design are obtained by means of the S/N ratio. Higher the S/N ratio, more stable the achievable quality. Figure 5.1 shows the S/N ratio plots for erosion. It is clear from Figure 5.1, highest S/N ratio first level of oxygen flow rate (300), the first level of fuel flow (55), the first level of spray angle (60). Therefore, the optimal setting of process parameters which yield minimum erosion is A1 B1 C1.

Table 5.7 Best Combination of Factor Levels

Factor	Affecting Mean		Affecting Variation	
	Contribution	Best Level	Contribution	Best Level
Oxygen Flow (OF)	Significant	Level-1 (300)	Significant	Level-1(300)
Fuel Flow (FF)	Significant	Level-1 (55)	Significant	Level-1 (55)
Spray angle (SA)	Significant	Level-1 (60)	Significant	Level-1 (60)

**5.4 OPTIMUM EROSION RATE:**

$$\mu = \bar{T} + (\bar{A}_1 - \bar{T}) + (\bar{B}_1 - \bar{T}) + (\bar{C}_1 - \bar{T})$$

Where  $\bar{T}$  = Overall mean of the response

$\bar{A}_1, \bar{B}_1, \bar{C}_1$  = Average values of response at the 1st level of parameters A and B and C (Table5.4) :

$$\mu = 19.01722 + (17.66167-19.01722) + (17.335-19.01722) + (18.3366-19.01722) = 15.30422$$

The 95% confidence interval of confirmation experiments ( $CI_{CE}$ ) and population ( $CI_{POP}$ ) are calculated by using the equation 5.1 and 5.2 as rewritten below for ready reference:

$$CI_{CE} = \sqrt{F_{\alpha}(1, f_e) V_e \left[ \frac{1}{n_{eff}} + \frac{1}{R} \right]} \dots\dots\dots 5.1$$

$$CI_{POP} = \sqrt{\frac{F_{\alpha}(1, f_e) V_e}{n_{eff}}} \dots\dots\dots 5.2$$

Where,  $F_{\alpha}(1, f_e)$  = The F-ratio at the confidence level of  $(1-\alpha)$  against DOF 1 and error degree of freedom  $f_e$ ,

$f_e$  = error DOF,

$$n_{\text{eff}} = \frac{N}{1 + [\text{DOF associated in the estimate of mean response}]}$$

$$n_{\text{eff}} = 9/[1+(2+2+2)] = 1.28$$

$$V_e = \text{error variance} = 0.73$$

$$F_{0.05}(1, 2) = 18.51 \quad [\text{Tabulated F value; Roy, 1990}]$$

$$\text{So, } CI_{\text{POP}} = \pm 3.249$$

$$CI_{\text{CE}} = \pm 3.88$$

Therefore, the predicted confidence interval for confirmation experiments is:

$$\mu - CI_{\text{CE}} \leq \mu \leq \mu + CI_{\text{CE}}$$

$$11.4242 \leq \mu \leq 19.18422$$

The 95% confidence interval of the population is:

$$\mu - CI_{\text{POP}} \leq \mu \leq \mu + CI_{\text{POP}}$$

$$12.055 \leq \mu \leq 18.553$$

## 5.5 ANALYSIS OF HARDNESS

The effects of control parameters i.e. Oxygen flow rate (OF), fuel flow rate (FF) and Spray angle (SA) on hardness were evaluated. Three repetitions for each of 9 runs were completed to calculate the hardness. Hardness of the specimens was calculated on Rockwell hardness Y scale.

Table 5.8 Result of Hardness with 3 trials for each

S. No.	Oxygen Flow (OF) (L/min)	Fuel Flow (OF) (L/min)	Spray Angle SA (degree)	Hardness (HR15)		
				Test- 1	Test- 2	Test- 3
1	300	55	60	72.8	72.2	72.5
2	300	65	75	74.2	73.6	73.9
3	300	75	90	76	76.2	76.1
4	350	55	75	79.2	79.8	79.5
5	350	65	90	78.2	77.6	77.9
6	350	75	60	82.2	81.6	81.9
7	400	55	90	78.8	78.8	78.8
8	400	65	60	81.4	80.8	81.1
9	400	75	75	83.4	82.6	83

## 5.6 CALCULATION OF SIGNAL TO NOISE RATIO FOR RESPONSE FACTORS

S/N ratio is a response which consolidates repetitions and the effect of noise levels into one data point. Analysis of variance of the S/N ratio is performed to identify the statistically significant parameters. The analyses of the experimental data were carried out using MINITAB 15 software, which is specially used for DOE applications. The experimental results were transformed into signal-to-noise (S/N) ratios. S/N ratio is defined as the ratio of the mean of the signal to the standard deviation of the noise. The S/N ratio indicates the degree of the predictable performance of a product or process in the presence of noise factors. The S/N ratio for hardness is of “Smaller the better” characteristic which can be calculated as logarithmic transformation of the loss function.

$$S/N = -10\log \{ \Sigma (Y^2)/n \}$$

Table 5.9 Calculation of S/N ratio for Response Factors (MINITAB Output)

Experiment No.	Oxygen Flow (OF) (L/min)	Fuel Flow (FF) (L/min)	Spray Angle (SA) (degree)	S/N Ratio	Mean
1	300	55	60	-37.2068	72.5
2	300	65	75	-37.3729	73.9
3	300	75	90	-37.6277	76.1
4	350	55	75	-38.0074	79.5
5	350	65	90	-37.8308	77.9
6	350	75	60	-38.2657	81.9
7	400	55	90	-37.9305	78.8
8	400	65	60	-38.1805	81.1
9	400	75	75	-38.3816	83.0

## 5.7 ANALYSIS OF HARDNESS FOR SPRAY PARAMETERS:

### 5.7.1) Effect of input factor on hardness

The S/N ratio for each level of spray parameters are summarized and referred to the average effects in response table of mean and S/N ratio. For hardness the calculation of S/N ratio follows “smaller the better” model. The S/N ratio for each level of spray parameters are summarized and referred to the average effects

Table 5.10 Response Table for S/N ratio (MINITAB Output)

Level	OF	FF	SA
1	-37.40	-37.71	-37.88
2	-38.03	-37.79	-37.92
3	-38.16	-38.09	-37.80
Delta	0.76	0.38	0.12
Rank	1	2	3

Table 5.11 Response Table for Mean (MINITAB Output)

Level	OF	FF	SA
1	74.17	76.93	78.50
2	79.77	77.63	78.80
3	80.97	80.33	77.60
Delta	6.80	3.40	1.20
Rank	1	2	3

### 5.7.2 Analysis of variance (ANOVA) of hardness

The purpose of analysis of variance (ANOVA) is to determine which spray parameters significantly affect the hardness. Table 5.5 the result of ANOVA analysis of signal to noise data. It is apparent that the P values of parameters oxygen flow rate (OF) and fuel (propylene) flow rate (FF) was less than  $P = 0.05$ , thus Oxygen flow rate (OF) and fuel flow rate (FF) factor mentioned above affect hardness significantly. The other factor spray angle for hardness response was insignificant. The percentage contribution of each factor is shown in table 5.5

Table 5.12 ANOVA for S/N Ratio (MINITAB output)

Source	DF	Seq SS	Adj SS	Adj MS	F	P	Percentage contribution
OF	2	0.99662	0.99662	0.49831	37.34	0.026	77.76
FF	2	0.23651	0.23651	0.11826	8.86	0.041	18.41
SA	2	0.02451	0.02451	0.01226	0.92	0.521	1.90
Residual Error	2	0.02669	0.02669	0.01335			
Total	8	1.28434	1.28434				

Table 5.13 ANOVA for Mean (MINITAB output)

Source	DF	Seq SS	Adj SS	Adj MS	F	P
OF	2	79.040	79.040	39.5200	42.49	0.023
FF	2	19.340	19.340	9.6700	10.40	0.058
SA	2	2.340	2.340	1.1700	1.26	0.443
Residual Error	2	1.860	1.860	0.9300		
Total	8	102.580				

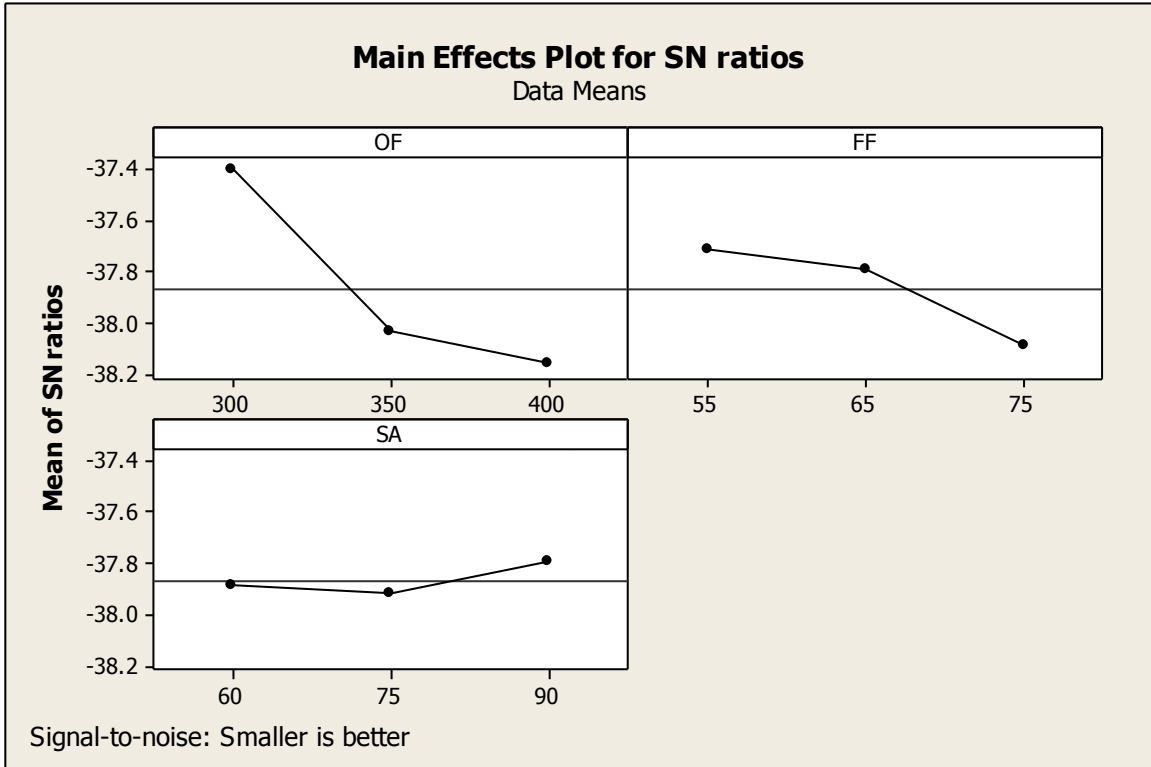


Figure 5.3 Main Effects plot for SN ratio

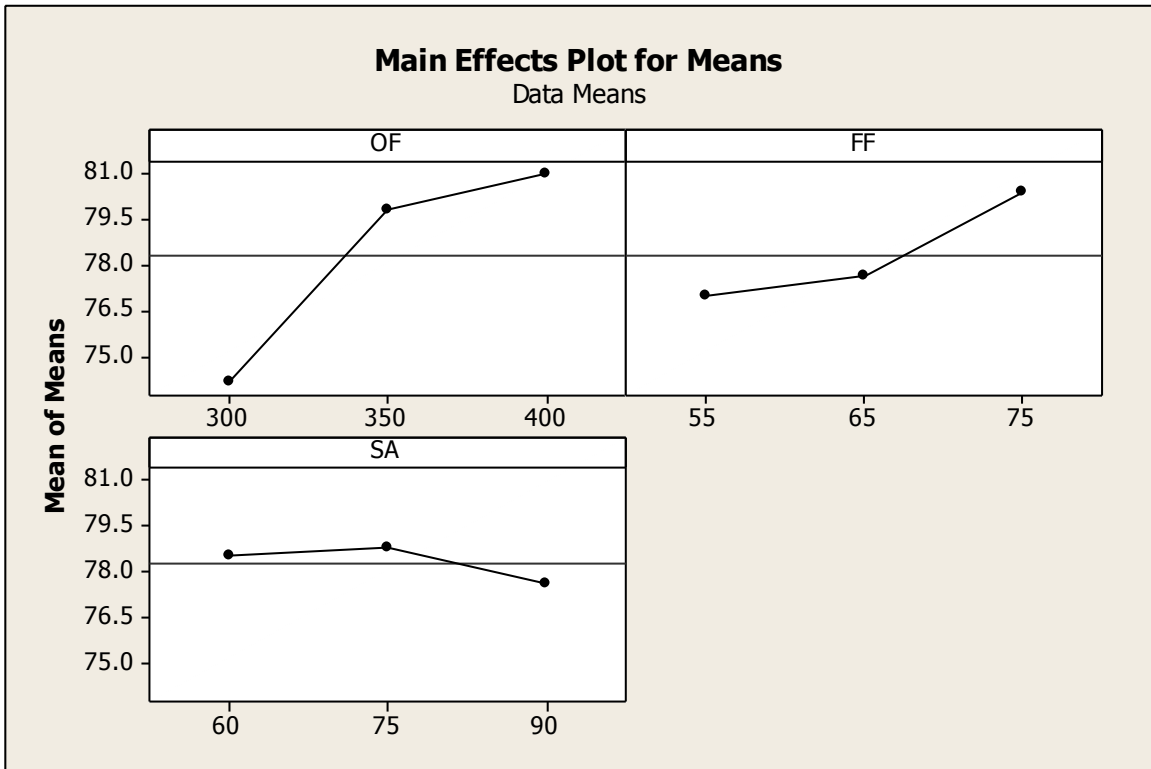


Figure 5.4 Main Effects plot for Data Means

The least variation and the optimal design are obtained by means of the S/N ratio. Higher the S/N ratio, more stable the achievable quality. Figure 5.3 shows the S/N ratio plots for hardness. It is clear from Figure 5.3, highest S/N ratio first level of oxygen flow rate (300) and fuel flow rate (55) and the other factor spray angle is insignificant. Therefore, the optimal setting of process parameters which yield minimum hardness is A1B1.

Table 5.14 Best Combination of Factor Levels

Factor	Affecting Mean		Affecting Variation	
	Contribution	Best Level	Contribution	Best Level
Oxygen Flow (OF)	Significant	Level-1 (300)	Significant	Level-1(300)
Fuel Flow (FF)	Significant	Level-1 (55)	Significant	Level-1 (55)
Spray angle (SA)	Insignificant	–	Insignificant	–

### 5.8 Optimum Hardness:

$$\mu = \bar{T} + (\bar{A}_1 - \bar{T}) + (\bar{B}_1 - \bar{T})$$

Where  $\bar{T}$  = Overall mean of the response

$\bar{A}_1, \bar{B}_1$  = Average values of response at the 1st level of parameters A and B and C (Table5.11)

$$\mu = 78.3 + (74.17-78.3) + (76.93-78.3) = 72.8$$

The 95% confidence interval of confirmation experiments ( $CI_{CE}$ ) and population ( $CI_{POP}$ ) are calculated by using the equation 5.3 and 5.4 as rewritten below for ready reference:

$$CI_{CE} = \sqrt{F_{\alpha}(1, f_e) V_e \left[ \frac{1}{n_{eff}} + \frac{1}{R} \right]} \dots\dots\dots 5.3$$

$$CI_{POP} = \sqrt{\frac{F_{\alpha}(1, f_e) V_e}{n_{eff}}} \dots\dots\dots 5.4$$

Where,  $F_{\alpha}(1, f_e)$  = The F-ratio at the confidence level of  $(1-\alpha)$  against DOF 1 and error degree of freedom  $f_e$ ,

$f_e$  = error DOF,

$$n_{\text{eff}} = \frac{N}{1 + [\text{DOF associated in the estimate of mean response}]}$$

$$n_{\text{eff}} = 9/[1+(2+2+2)] = 1.28$$

$$V_e = \text{error variance} = 0.012803$$

$$F_{0.05}(1, 2) = 18.51 \quad [\text{Tabulated F value; Roy, 1990}]$$

$$\text{So, } CI_{\text{POP}} = \pm 0.430$$

$$CI_{\text{CE}} = \pm 0.551$$

Therefore, the predicted confidence interval for confirmation experiments is:

$$\mu - CI_{\text{CE}} \leq \mu \leq \mu + CI_{\text{CE}}$$

$$72.249 \leq \mu \leq 73.351$$

The 95% confidence interval of the population is:

$$\mu - CI_{\text{POP}} \leq \mu \leq \mu + CI_{\text{POP}}$$

$$72.37 \leq \mu \leq 73.23$$

## 5.9 EXPERIMENTAL VALIDATION

In order to validate the results obtained, two confirmation experiments were conducted for each of the tribological characteristics (erosion rate and hardness) at optimal levels of the process variables. The average values of confirmation results have been compared with the predicted values. The results are listed in Table 5.15. The values of wear rate and erosion rate are obtained through confirmation experiments are within the 95% of  $CI_{\text{CE}}$  of respective tribological characteristic. It is to be pointed out that these optimal values are within the specified range of process variables.

Table 5.15 Predicted Optimal Values, Confidence Intervals and Results of Confirmation Experiments

<b>Tribological Characteristics</b>	<b>Optimal set of parameters</b>	<b>Predicted Optimal Value</b>	<b>Predicted Confidence Interval at 95% confidence level.</b>	<b>Actual Value (average of two confirmation experiments)</b>
Erosion rate	A1B1C1	15.304	$12.05 \leq \mu \leq 18.55$	15.380
Hardness	A1B1C1	72.8	$72.37 \leq \mu \leq 73.23$	72.67

## 5.10 DISCUSSION

The O/F ratio is a very important parameter and can greatly affect the coating quality. During the HVOF process, the feedstock particles are injected into the high velocity hot gas generated through combustion of oxygen and a fuel gas. The oxygen flow rate affects the combustion reaction. Combustion temperature depends on the stoichiometry of the oxygen fuel mixture. O/F ratio is too low; the flame temperature will not be high enough to insure the particles to obtain enough energy thus the melting condition of feedstock will be worse resulting in low hardness of coatings due to these unmelted particles. With the increase of oxygen flow rate, the fuel is combusted more completely, resulting in the higher particle temperature. The flame temperature reaches a maximum value, when the oxygen content is enough to produce the complete combustion of propylene (fuel) and all the particles at this stage would be in the liquid phase when impacting the substrate resulting the maximum hardness and erosion resistance of coating. An excess of oxygen will cool the flame decreasing the particle temperature and can also lead to the oxidation of the particles, since the completely melted particles exposed to the high temperature atmosphere will react with oxygen further. For higher oxygen flow rate values, there will be an excess of oxygen that acts as cooling gas and consequently promotes a flame temperature decrease. Secondly, the increase in total gas flow rate increases the particle velocity, reducing the residence time of the particle into the flame, and consequently decreasing the particle temperature causing the unmelted particles impacting on surface resulting in low hardness and less erosion resistance.

**6.1 CONCLUSION**

In present work, effect of various factors (oxygen flow rate, propylene flow rate, spray angle) in HVOF spraying were studied for the maximization of erosion resistance and minimization of hardness using Taguchi's parameter design. The analysis shown that the factors like oxygen flow rate (OF), fuel (propylene) flow rate (FF), and spray angle (SA) plays significant role in erosion resistance and factors oxygen flow rate (OF), fuel (propylene) flow rate (FF) plays significant role in hardness. Analysis of results leads to conclusion that factors at level A1, B1, C1 can be set for maximum erosion resistance and factors A1, B1 for minimum hardness.

**6.2 SCOPE FOR FUTURE WORK**

In present analysis we used Taguchi and ANOVA optimization technique, in future other techniques like Genetic algorithms, Finite elements method, artificial neural network analysis etc. can be used for the rectification and optimization of the results. For coating other techniques can be used like plasma spray, arc spraying, electroplating etc. Erosion behaviour of abradable coating can be compared by using more than two techniques at a time.

## REFERENCES

---

- [1] **Ashok K. Vijh**, “Comparative tendencies for metal loss by abrasive wear, impact erosion and arc erosion”, *Wear*, 49 (1978) 141-145.
- [2] **Thomas E. Strangman**, “Thermal barrier coatings for turbine airfoils”, *Thin solid films*, 127 (1985) 93-105
- [3] **J.E.RESTALL, D.J.Stephenson**, “High temperature erosion of coated superalloys of gas turbine”, *Material Science and Engineering*, 88(1987) 273-282.
- [4] **S.Turenne,M.Fiset,J.Masounave**, “The effect of sand concentration on the erosion of materials ay a slurry jet”, *Wear*,133 (1989) 95-106.
- [5] **T.N.Rhys-Jones**,“The use of thermally sprayed coatings for compressor and turbine applications in aero engines”,*Surface and coating technology*, 42 (1990) 1-11.
- [6] **Randall S.Lynn, Kien K.Wong, Hector Mcl.Clark**, “On the particle size effect in slurry erosion”, *Wear*,149 (1991) 55-71.
- [7] **I.Swadzba, B.Formanek, H.M.Gabriel,P.Liberski,P.Podoloski**,“Erosion and corrosion resistant coatings for aircraft compressor blades”, *Surface and coating technology*, 62 (1993) 486-492
- [8] **K.T. Kembaiyan, Kesh Keshavan**, “Combating severe fluid erosion and corrosion of drill bits using thermal spray coatings”, *Wear*, 186-187 (1995) 487-492.
- [9] **W.Tabakoff, V.Shanov**, “Erosion rate testing at high temperature for turbomachinery use”, *Surface and coatings technology*, 76-77 (1995) 75-80.
- [10] **P.Fauchais, M.Vardelle, A.Vardelle, L.Bianchi**, “Plasma Spray:Study of the coating generation”, *Ceramics International*, 22 (1996) 295-303.
- [11] **Yi Maozhong, Zhang Xianlong, Ji Gengshun, He Jiawen**, “Evaluation of Al-Si/Polyster abradable seal coating”, *Trans. Nonferrous Met. Soc. China* Vol.6, No.4, (1996).
- [12] **Peter J.Blau**, “Fifty years of research on the wear of metals”, *Tribology International* Vol. 30, No.5, (1997) 321-331.
- [13] **John T. Burwell**, “Survey of possible wear mechanisms”, *Wear*,Vol.1, 76-77 (1997) 119.

- [14] **Erich Lugscheider, Christian Herbst, Lidong Zhao**, “Parameter studies on high-velocity oxy-fuel spraying of MCrAlY coatings”, *Surface and coatings technology*, 108-109 (1998) 16-23.
- [15] **I.M.Hutchings**, “Abrasive and erosive wear tests for thin coatings: a unified approach”, *Tribology International* Vol. 31, No’s 1-3 (1998) 5-15.
- [16] **L.C.Erickson, T.Troczyński, H.M.Hawthorne, H.Tai, D.Ross**, “Alumina coating by plasma spraying of monosize sapphire particles”, *ASM International*, Vol. 8(3) (1999) 421-426.
- [17] **Maozhong Yi, Jiawen He, Baiyun Huang, Huijiu Zhou**, “Friction and wear behaviour and sbradability of abradable seal coating”, *Wear*, 231(1999) 47-53.
- [18] **J.A.Hearley, J.A.Little, A.J.Sturgeon**, “The effect of spray parameters on the properties of high velocity oxy-fuel NiAl intermetallic coatings”, *Surface and coatings technology*, 123 (2000) 210-218.
- [19] **J.A.Hearley, J.A.Little, A.J.Sturgeon**, “The erosion behavior of NiAl intermetallic coatings produced by high velocity oxy-fuel thermal spraying”, *Wear*, 233-235 (1999) 328-333.
- [20] **Bu Xian Wang, Zheng Rong Shui**, “The hot erosion behavior of HVOF chromium carbide-metal cermet coatings sprayed with different powders”, *Wear*, 253 (2002) 550-557.
- [21] **M.P.Planche, B.Normand, H.liao, G.Rannou, C.Coddet**, “Influence of HVOF spraying parameters on in-flight characteristics of Inconel 718 particles and correlation with the electrochemical behavior of the coating”, *Surface and coatings technology*, 157 (2002) 247-256.
- [22] **C.R.C.Lima, F.Camargo**, “Evaluation of HVOF coatings for wear applications”, *Thermal Spray*, (2003) 763.
- [23] **Lidong Zhao, Matthias Maurer, Falko Fischer, Robert Dicks, Erich Lugscheider**, “Influence of spray parameters on the particle in-flight properties and the properties of HVOF coating of WC-CoCr”, *Wear*, 257 (2004) 41-46.
- [24] **T.S.Sidhu, S.Prakash, R.D.Agrawal**, “Studies on the properties of High-Velocity Oxy Fuel thermal spray coatings for higher temperature applications”, *Materials Science*, Vol. 41, No. 6 (2005) 805.

- [25] **H.I.Faraoun, T.Grosdidier, J.L.Seichepine, D.Goran, H.Aourag, C.Coddet J.Zwick,N.Hopkins**, “Improvement of thermally sprayed abrasible coating by microstructure control”, *Surface and coatings technology*, 201(2006) 2303-2312.
- [26] **Xio Ma,Allan Matthews**, “Investigation of abrasible seal coating performance using scratch testing”, *Surface and coatings technology*, 202 (2007) 1214-1220.
- [27] **M.Gaona,R.S.Lima,B.R.Marple**, “Influence of particle temperature and velocity on the microstructure and mechanical behavior of HVOF sprayed nanostructured titania coatings”, *Journal of material processing technology* , 198 (2008) 426-435.
- [28] **M.Hasan,J.Stokes,L.Looney,M.S.J.Hashmi**, “Effect of spray parameters on residual stress build-up of HVOF sprayed aluminium/steel functionally graded coatings”, *Surface and coatings technology*, 202 (2008) 4006-4010.
- [29] **Adnan Al-Bashir, A.K.Abdul Jawwad,Khalil Abu Shgair**, “Evaluating the effects of spray parameters on wear resistance of steel-shaft material”, *Jordan journal of mechanical and industrial engineering*, Volume 3,No. 2 (2009) 157-160.
- [30] **S.S.Mahapatra, Amar Patnaik**, “Study on mechanical and erosion wear behavior of hybrid composites using Taguchi experimental design”, *National Conference on Advancements and Futuristic Trends in Mechanical and Materials Engineering* (2010) 45.
- [31] **D.P.Kashyap, T.S.Sidhu, S.Prakash**, “Parametric effect of HVOF process on erosion corrosion behavior of coatings-A Review”, *Materials and Design* 30 (2009) 2791-2801
- [32] **Christophe Lyphout, Per Nylen, Lars Ostergren**, “Relationships between process parameters, microstructure and adhesion strength of HVOF sprayed IN718 coatings”, *ASM International*, (2010) 76-82.
- [33] **Maria Oksa,Erja Turunen,Tomi suhonen,Tommi Varis,Semo-Pekka Hannula**, “Optimization and characterization of High Velocity Oxy-fuel Sprayed coatings: Techniques, Materials and applications”, *Coatings*,1, (2011) 17-52.
- [34] **Y.Wang, S.L.Jiang, Y.G.Zheng, W.Ke, W.H.Sun, X.C.Chang, W.L.Hou, J.Q.Wang**, “Effect of processing parameters on the microstructures and corrosion behavior of HVOF sprayed Fe-based amorphous metallic coatings”, *Materials and corrosion*, 63,No. 9999 (2012).
- [35] **Sarka Houdkova, Michaela Kasparova,Jan Schubert**, “The spraying parameters optimization of the HVOF STELLITE 6 coating”, *METAL* 2012, (2012) 23-25.

[36] **Yi Maozhong, Huang Baiyun, He Jiawen**, “Erosion wear behavior and model of abradable seal coating”, *Wear* 252 (2012) 9-15

[37] **A.J.Lopez, B.Torres, C.Taltavull**, “Influence of high velocity oxygen-fuel spraying parameters on the wear resistance of Al-SiC composite coatings deposited on ZE41A magnesium alloy”, *Materials and design*, 43 (2013) 144-152.

[38] **D.Sudhakra, DR.G.Prasanthi**, “Effect of machining parameters on metal removal rate of VANADIS 4E with WEDM by Taguchi method”, *International journal of emerging trends in engineering and development*, Issue 3, Vol. 1 (2013).

103 (2000), 288-292